

**Thin shell foundations:
Embodied carbon reduction through materially efficient geometry**

by

Kiley Anne Feickert

Bachelor of Architecture
California Polytechnic University, San Luis Obispo, 2013

Submitted to the
Department of Architecture
In partial fulfilment of the requirements for the degree of

MASTER OF SCIENCE IN ARCHITECTURE STUDIES
AT THE
MASSACHUSETTS INSTITUTE OF TECHNOLOGY

MAY 2022

©2022 Kiley Anne Feickert. All rights reserved.

The author hereby grants to MIT permission to reproduce and to distribute publicly paper and electronic copies of this thesis document in whole or in part in any medium now known or hereafter created.

Signature of Author
Department of Architecture
May 06, 2022

Certified by
Caitlin T. Mueller
Associate Professor of Architecture and Civil and Environmental Engineering
Thesis Supervisor

Accepted by
Leslie K. Norford
Professor of Building Technology
Chair, Department Committee on Graduate Student

Thesis Committee:

THESIS SUPERVISOR

Caitlin T. Mueller, PhD
Ford International Career Development Professor
Associate Professor of Architecture
Associate Professor of Civil and Environmental Engineering
Massachusetts Institute of Technology

& READER

Sigrid Adriaenssens, PhD
Associate Professor of Civil and Environmental Engineering
Director, Program in Mechanics, Materials and Structures
Princeton University

Thin shell foundations: Embodied carbon reduction through materially efficient geometry

by

Kiley Anne Feickert

Submitted to the Department of Architecture
on May 19, 2022 in partial fulfillment of the requirements for the degree of
Master of Science in Architecture Studies

ABSTRACT

Due to increasing global population, floor area is expected to double by 2060. At the same time, the building sector contributes 11% of global greenhouse gas emissions annually as a result of current construction processes. Therefore, if global warming is to be limited to 1.5°C above pre-industrial levels, reducing embodied carbon will play a key role and business-as-usual construction processes must be reconsidered. This research aims to reduce carbon emissions associated with reinforced concrete structural elements while addressing the need for a significant increase in adequate housing due to rapid urbanization.

The structural floor system, frame and foundations represent the systems with the most potential to limit emissions, as they are the biggest contributors to embodied carbon in a building. In contexts where labor costs drive construction costs, particularly in the Global North, material is consumed excessively at the expense of time. This research proposes shell foundations in lieu of spread foundations, drawing from historical applications such as Félix Candela's Customs Warehouse, built in 1953. Shells distribute loads more efficiently through their cross-section, reducing the quantity of material required structurally which ultimately reduces their embodied carbon.

In this research, existing analytical equations are applied in a parametric design workflow to evaluate the environmental impact of conventional prismatic foundations and shell foundations for the same design load. For a 2MN column load on clay soil, shells reduce embodied carbon in foundations by 48%. By applying this approach systematically, insights are gained regarding their applicability to various building typologies and site conditions. For high applied loads, and soils with low bearing capacity, shells significantly outperform their prismatic counterparts. Foundations are then considered within the context of a whole building to determine the potential downstream savings when multiple systems are shape optimized. When floor slabs are shape-optimized in addition to using shell foundations, the embodied carbon of a building can be reduced by 72%.

Digital fabrication offers a pathway to economically build materially efficient foundations while addressing the additional time and labor often associated with more complex geometry. For example, advances in 3D printing earth suggest local soil can act as formwork if printed in the required shape to receive the shell geometry. Additionally, subtractive methods are explored, where earth is compacted and milled to create formwork for a shell foundation.

Thesis Supervisor: Caitlin T. Mueller

Title: Associate Professor of Architecture and Civil and Environmental Engineering

ACKNOWLEDGEMENTS

Thank you to everyone that has contributed to this research. First and foremost, I want to thank my thesis supervisor, Professor Caitlin Mueller, who this work would not have been possible without. Thank you for encouraging me to be critical of business-as-usual practices in order to make a positive contribution to our field. Your mentorship and guidance have been invaluable and I'm incredibly grateful for your time, support, and encouragement in taking on topics that were beyond my expertise. I look forward to expanding this work with you.

Thank you to the Building Technology faculty – Professors Caitlin Mueller, Christoph Reinhart, John Ochsendorf, Leon Glicksman and Leslie Norford – for creating a space that focuses on building a more sustainable and equitable future. I appreciate the community you've created and it's been a privilege learning from all of you. Thank you for engaging with and providing feedback on this research as well as inspiring me to consider building technology more holistically. I'm grateful to Professor Sigrid Adriaenssens, for being a reader for this thesis. Thank you for your feedback, expertise and encouragement. Stacy Clemons, I appreciate all of your support throughout my time in the lab so far, thank you. I'm also grateful to MIT professor Andrew Whittle for generously sharing his expertise and insights in geotechnical engineering as this research was developed.

I feel extremely fortunate to work with all of my BT lab mates, and in particular the members of the Digital Structures Research Group, Ashley Hartwell, Demi Fang, Eduardo Gascón Alvarez, Keith J. Lee, Lavender Tessmer, Leilah Sory, Mohamed Ismail, Ramon Weber, Sandy Curth, and Yijiang Huang, as well as Ellen Reinhard, Juliana Berglund-Brown, Laura Gonzalez, Nada Tarkhan, Sarah Mokhtar and Sloan Aulgur. I appreciate learning from you through all of our discussions and collaborations. Thank you for your feedback and friendship through the development of this work.

It's been a pleasure working with Q Rael, Chris Dewart, Taylor Boes, Gil Sunshine, and Stephen Rudolph on the fabrication aspects of this research. I greatly appreciate your time and insights throughout the entire process.

Thank you to Professors Robert Arens and Thomas Fowler and colleagues and collaborators Leon Rost and David Illingworth for helping me reach MIT.

To my Mom, Dad, Casey, Katie, Malia, Cadence and Katarina, I can't understate my appreciation for your love and support. We did it.

Funding for this research was provided by the Dar Group Urban Seed Grant Program at the Norman B. Leventhal Center for Advanced Urbanism, Massachusetts Institute of Technology.

CONTENTS

ABSTRACT	5
ACKNOWLEDGEMENTS	6
1.	9
INTRODUCTION.....	9
1.1. ENVIRONMENTAL IMPACT OF REINFORCED CONCRETE STRUCTURES	10
1.1.1. DEFINITION OF EMBODIED CARBON	10
1.1.2. EMBODIED CARBON OF STRUCTURAL MATERIALS	11
1.1.3. REINFORCED CONCRETE.....	12
1.1.4. EMISSION REDUCTION STRATEGIES	13
1.2. ENVIRONMENTAL IMPACT OF FOUNDATIONS	13
1.3. OPPORTUNITIES.....	14
2.	15
LITERATURE REVIEW.....	15
2.1. CONCRETE STRUCTURAL DESIGN OPTIMIZATION.....	15
2.1.1. FOUNDATION OPTIMIZATION	16
2.2. EFFICIENT OR INNOVATIVE FOUNDATIONS THROUGH GEOMETRY	17
2.3. SHELL FOUNDATION ENGINEERING.....	19
2.3.1. SELECT CONTRIBUTORS TO SHELL FOUNDATION ENGINEERING	19
2.3.2. SUMMARY OF PREVIOUS INVESTIGATIONS ON SHELL FOUNDATIONS.....	20
2.4. OPPORTUNITIES FOR DIGITAL FABRICATION FOR SHELL FOUNDATIONS	22
2.5. RESEARCH GAP AND RESEARCH QUESTIONS.....	24
3.	25
METHODOLOGY	25
3.1. COMPUTATIONAL DESIGN SPACE OF FOUNDATIONS	25
3.1.1. CONCEPTUAL OVERVIEW	25
3.1.2. STRUCTURAL DESIGN OF SPREAD FOOTINGS	27
3.1.3. STRUCTURAL DESIGN OF SHELL FOOTINGS	29
3.1.4. EMBODIED CARBON CALCULATION	31
3.2. WHOLE BUILDING FRAME ANALYSIS	33
4.	34
EXPERIMENTS / RESULTS	34
4.1. SINGLE ELEMENT COMPARISONS	34
4.1.1. EMBODIED CARBON COMPARISON OF SPREAD FOOTINGS VERSUS SHELL FOOTINGS...34	
4.1.2. APPLICABILITY OF SHELLS TO VARIOUS CONTEXTS	36
4.1.3. NORMALIZED EMBODIED CARBON BY FOUNDATION TYPE AND FLOOR BUILD-UP IN CLAY SOIL.....	40
4.2. WHOLE BUILDING FRAME ANALYSIS	41
4.2.1. IMPACT OF SHAPE-OPTIMIZING STRUCTURAL ELEMENTS ON GLOBAL WARMING POTENTIAL	41

4.2.2. IMPACT OF CONCRETE STRENGTH ON REDUCING BUILDING FRAME GWP	42
5.	44
DIGITAL FABRICATION EXPERIMENTS	44
5.1. CONCEPTS.....	44
5.2. METHODS.....	44
5.2.1. CLAY EXTRUSION.....	44
5.2.2. ADOBE MILLING	46
5.3. DIGITAL FABRICATION CONCLUSION.....	49
6.	50
CONCLUSION	50
6.1. SUMMARY OF CONTRIBUTIONS.....	50
6.2. POTENTIAL IMPACT.....	50
6.3. LIMITATIONS AND FUTURE WORK.....	51
6.4. CONCLUDING REMARK	51
REFERENCES.....	52

1. INTRODUCTION

Due to increasing global population, floor area is expected to double by 2070 (Energy Technology Policy Division 2021). At the same time, the embodied carbon of the building sector (the emissions associated with constructing buildings) contributes at least 11% of global greenhouse gas emissions annually (Adams, Burrows, and Richardson 2019). Reducing carbon emissions associated with buildings will play a critical role in limiting global warming to 1.5°C above pre-industrial levels and creating a more equitable future. However, in order to provide adequate housing for the rising global population, it will be necessary to build more. Additionally, the accessibility and prevalence of concrete requires that the building industry find ways to use less of it, especially in locations where low carbon materials are not locally available for substitution. Therefore, it's vital to reconsider business-as-usual construction methods in order to build more efficiently.

The structural floor system, frame, and foundations are the biggest contributors to embodied carbon in a building (Adams, Burrows, and Richardson 2019) and thus represent the systems with the most potential to limit emissions. For midrise nonresidential projects, for example, the super- and sub-structure account for over 50% of the building's total embodied carbon (Kaethner and Burrige 2012). In reinforced concrete floors and frames, most of this material is not required structurally, but is used for ease of construction as building methods have trended toward simplicity at the expense of material efficiency. This is particularly true in contexts where labor costs drive construction costs, such as the Global North, since prismatic elements are faster to build than elements that have more complex geometry.

However, by utilizing reinforced concrete only where it's required structurally, architects and engineers have demonstrated that significant material and carbon savings can be achieved. Abundant examples have been studied in visible structural elements such as roofs, floor slabs, and beams (Ismail and Mueller 2021) (Orr et al. 2019) (Block et al. 2017) (Sec. 2.1). However, foundations are a highly impactful and highly understudied (Afzal et al. 2020) contributor to a building's embodied carbon emissions accounting for up to 40%, and 27% on average (Pratt 2016). This highlights the opportunity to design more materially efficient substitutions to typical foundation systems.

Taking inspiration from history, thin, reinforced concrete shells are proposed in lieu of spread footings due to their ability to distribute loads more efficiently through their cross-section. Shells utilize membrane action rather than bending which reduces the quantity of material required structurally (Williams 2014). Historical examples are presented to demonstrate their ability to save material and improve geotechnical performance, beginning with Félix Candela's first known modern example, constructed in Mexico in 1953 (Abdel-Rahman 1996). The most significant example of material savings was found to be up to 72% compared to a conventional raft foundation, while other projects achieved a savings of up to 50% (Abdel-Rahman 1996).

Shells are materially efficient due to their complex curvature which has hindered their implementation in contexts where skilled labor costs outweigh material costs. However, the significant reduction in embodied carbon urges the building industry to confront the challenges to fabricate shell foundations. Additionally, contemporary digital fabrication techniques such as 3D printing or milling earth may offer an economical pathway to achieving more complex shapes while mitigating the need for additional labor or expense. This research aims to reduce carbon emissions associated with reinforced concrete foundations by utilizing efficient shell geometry and proposes digital fabrication to build them economically.

1.1. ENVIRONMENTAL IMPACT OF REINFORCED CONCRETE STRUCTURES

This section provides a definition of embodied carbon in order to establish a common language for the following experiments. The environmental impact and prevalence of reinforced concrete is discussed in relation to other structural materials as well as the carbon emissions associated with business-as-usual foundation design.

1.1.1. DEFINITION OF EMBODIED CARBON

The environmental impact of constructing a building is often described as its *embodied carbon* (EC). For the purpose of this work, embodied carbon is measured in units of carbon dioxide equivalence (CO₂e), which represent the *global warming potential* (GWP) of the greenhouse gases emitted through various industrial processes. For example, a kilogram of carbon dioxide has a global warming potential of 1 kg CO₂e. Embodied carbon can be defined as the cumulative carbon emissions (CO₂e) associated with the processes required to produce a building. It is a historical fact, not a material property. This includes all emissions from extracting and transporting raw materials, manufacturing building materials, transporting them to site, and construction, summarized as the *upfront carbon* (See Fig. 1) (Adams, Burrows, and Richardson 2019).

Embodied carbon can also include material refurbishment and replacement during the use stage of a building, as well as emissions as a result of demolition, transportation, waste processing and disposal at the end of a buildings life (Adams, Burrows, and Richardson 2019). However, these emissions have not been considered in this work due the fact that these processes do not fall within an architect and structural engineers' scope at the design stage of a project. Additional key terms relating to embodied carbon are shown in Figure 1 which align with the European standard EN 15978.

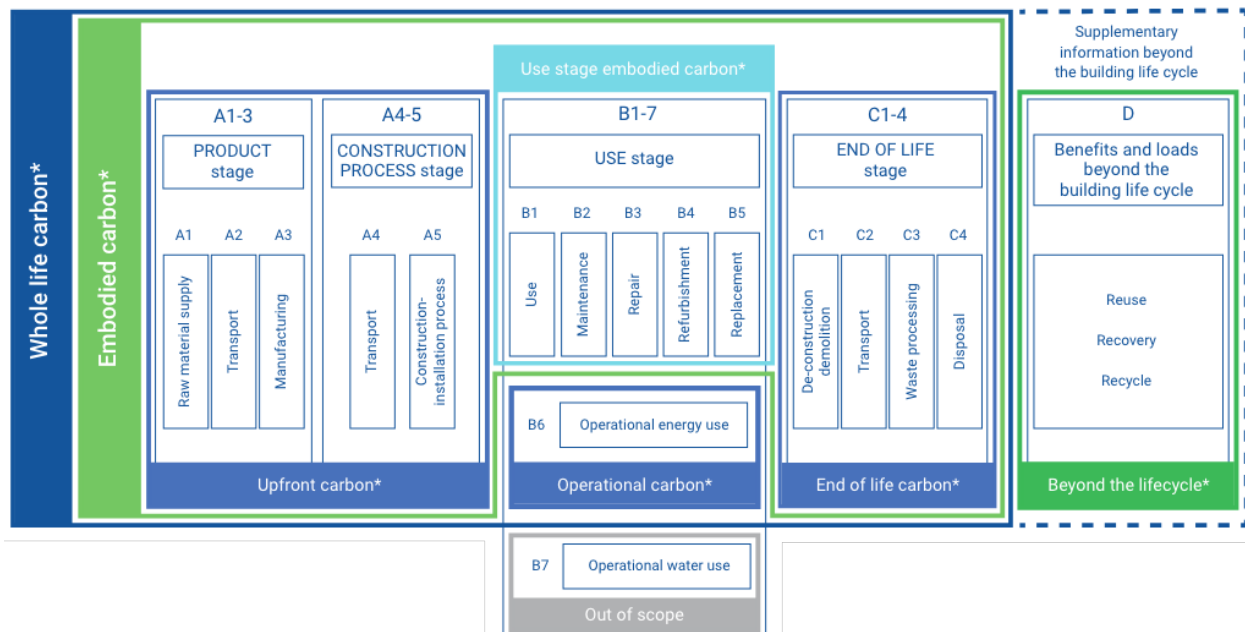


Figure 1: Key terms and stages of embodied carbon in buildings (Adams, Burrows, and Richardson 2019)

In this research, embodied carbon is used interchangeably with global warming potential which is calculated by multiplying the structural material quantity required to support a given load by the embodied carbon coefficient for the respective material (See Sec. 1.1.2). There is a misconception

that embodied carbon only relates to cement, however every material used in construction requires extraction, transportation and processes to manufacture and each of these steps is responsible for emitting carbon dioxide or equivalent greenhouse gases into the atmosphere. The embodied carbon coefficients used in this research come from the Inventory of Carbon and Energy (ICE) database (V3.0 2019) (Hammond and Jones 2008).

1.1.2. EMBODIED CARBON OF STRUCTURAL MATERIALS

The global warming potential of different structural materials varies considerably due to the processes required to produce them and their respective material properties. The allowable tensile and compressive stresses and buckling capacities of mass timber, structural steel and reinforced concrete vary substantially requiring more or less material in various applications. For example, the cross sections required for a beam in each material to span 20ft supporting a typical load in bending is shown in Figure 2. Due to the carbon density per strength of the materials, the global warming potential ranges from 1.0 kgCO_{2e} for mass timber, to 1.8 kgCO_{2e} for reinforced concrete, with a steel section accounting for 1.5 kgCO_{2e} (See Table 1).

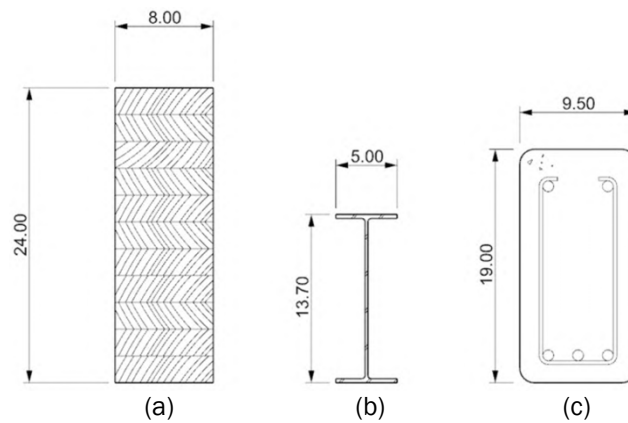


Figure 2: Equivalent cross-section to support the same load in (a) mass timber, (b) steel, and (c) reinforced concrete (Fang et al. In preparation)

Table 1: Global warming potential for beams of various structural materials designed to span 20ft (Fang et al. In preparation) *values from ICE database V3.0 2019 (Hammond and Jones 2008)

Material	Embodied Carbon Coefficient* (kgCO _{2e} /kg)	Structural Material Quantity (kg)	Global Warming Potential (kgCO _{2e})
Glue-laminated timber	0.49	400	1.0
Wide flange steel	1.55	190	1.5
Reinforced concrete	0.14	2630	1.8

While substitution of low carbon materials such as mass timber is encouraged in contexts where these materials are locally available, substitution will not be possible in all contexts. In addition, even if the cement and steel industries are decarbonized, the raw materials required for their creation are finite and consumption is expected to rise substantially in the coming years. This suggests that developing methods for using less reinforced concrete initially will be a key component in reducing building sector carbon emissions.

1.1.3. REINFORCED CONCRETE

Reinforced concrete (RC) structures are composite systems comprised of a large volume of reinforcing steel and concrete. For example, construction accounts for over half the world's steel consumption and steel reinforcing bars for making reinforced concrete are the single largest application (Allwood and Cullen 2015). Due to the processes required to manufacture them, both materials have a high ecological impact in terms of their carbon emissions and their consumption of nonrenewable resources.

Concrete is made by mixing water, cement, and aggregate (sand or gravel). Cement production alone contributed approximately 8% of anthropogenic CO₂ emissions in 2012 (Miller et al. 2018) with demand expected to increase by 75% by 2050 (Allwood and Cullen 2015). There is currently no recycling route for cement (unlike other industries such as steel and aluminum) due to the inability to reverse the chemical reaction that the material undergoes when concrete is created (Allwood and Cullen 2015). Rather, concrete components are typically down-cycled by crushing them into aggregate. This alleviates demand on aggregate shortages and diverts concrete from being landfilled. However, conventional aggregate has 25 times less embodied carbon than down-cycled concrete aggregate, which also requires additional cement if it is to be reformed into concrete (Allwood and Cullen 2015). Some would argue that concrete should only be used in rare circumstances due to its environmental impact. However, reinforced concrete has and will continue to be a key component in the sovereign development of countries around the world (Ismail and Mueller 2022) and, therefore, should not be ruled out as a building material in all contexts.

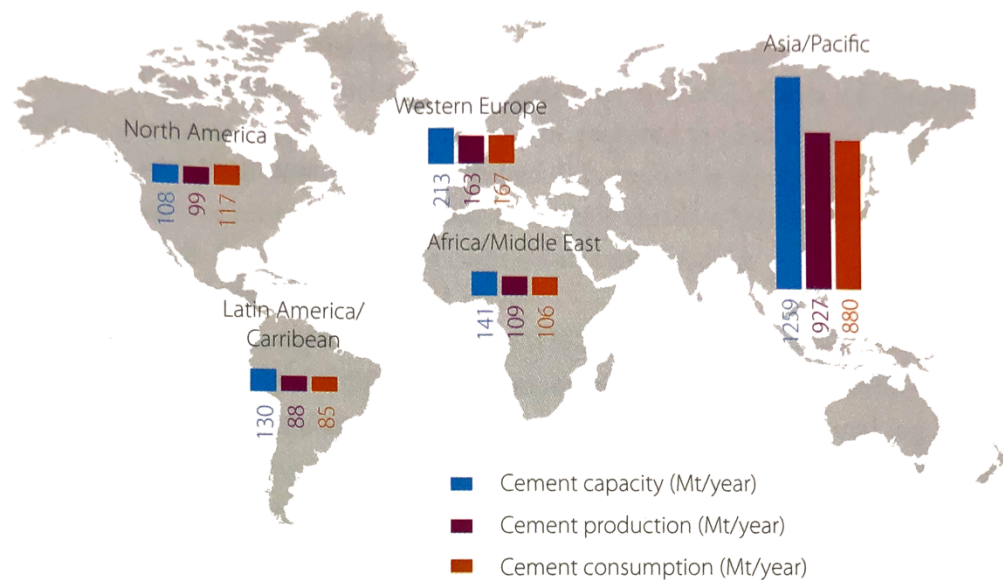


Figure 3: “Global cement capacity, production and consumption” (Allwood and Cullen 2015)

Domestic housing is typically the second highest end-use of reinforced concrete after infrastructure, followed by the remaining building types split evenly (Allwood and Cullen 2015). One of the main reasons concrete is used ubiquitously throughout the globe is that the raw materials to make cement (along with the other constituent ingredients of concrete) are well distributed (See Fig. 3). It also has low value by weight, so little cement is traded internationally (Allwood and Cullen 2015). Due to the accessibility and prevalence of concrete, particularly in rapidly urbanizing areas, the building industry must find ways to use less of it.

1.1.4. EMISSION REDUCTION STRATEGIES

The building industry has signaled that it aims to reduce carbon emissions to meet climate goals. For example, the Structural Engineering Institute of the American Society of Civil Engineers has developed the Structural Engineers 2050 Commitment Program (SE 2050), which recognizes the need to eliminate embodied carbon by 2050. In 2021, the program had 55 signatory firms with 25 submitting Action Plans for reducing carbon emissions in their design practices. However, the methods for achieving this target are less well established than the intention. In a white paper by the Structural Engineering Institute’s Sustainability Committee Carbon Working Group, a modest saving of 10-25% was estimated as achievable through design optimization with carbon sequestration and carbon offsets accounting for a large percentage of reduction in some scenarios (“Achieving Net Zero Embodied Carbon in Structural Materials by 2050” 2020).

The American Institute of Architects (AIA) also established the AIA 2030 Commitment program in 2009 to encourage architecture practices to reach carbon neutral building performance by 2030 (American Institute of Architects 2021). This plan focuses on operational energy targets with embodied carbon as an optional metric. In 2019, of the 682 signatory firms, 311 had reported data on their projects and only 15 companies achieved the 80% predicted Energy Use Intensity reduction target. In both programs, the obligation of firms to meet the established targets is optional and the lack of market incentives for reducing material consumption have limited embodied carbon reduction in the construction industry in the United States.

For reinforced concrete buildings specifically, the IPCC 2014 Report on Industry identifies two pathways to reduce carbon emissions associated with them; “using less cement initially and reusing concrete components at end of first product life” (Fischedick et al. 2014). Using less cement initially can be achieved through; 1) substitution of lower energy intensive materials; and 2) using less concrete to satisfy the same design load. This thesis focuses on the last item, by quantifying how much less concrete can be used in foundations while providing the same floor area.

1.2. ENVIRONMENTAL IMPACT OF FOUNDATIONS

In a study of 200 buildings, reinforced concrete foundations accounted for 27.3% of a building’s total embodied carbon, on average, with the upper quartile of the data contributing 41% (See Table 2) (Pratt 2016). This study was based on built, medium to large-scale projects and actual material take-offs of the built project.

Table 2: Embodied carbon contribution from foundations and embodied carbon normalized by GFA for buildings surveyed, adapted from (Pratt 2016)

	EC Contribution from Foundation (%)		Normalized Embodied Carbon (kgCO₂e/m²)
Average	27.3	Average	170.3
Lower quartile	10	Minimum	9.5
Median	16	Median	76.6
Upper quartile	41	Maximum	918.2

Although this study provides a valuable baseline to understand the significance of foundations' contribution to carbon emissions, no data on geology, allowable settlement, or foundation typology is available, limiting the ability to analyze why these foundations are so materially intensive. Additionally, no single family residential projects were included in the analysis which account for approximately 79% of the total floor area and 61% of the estimated embodied carbon of the existing U.S. building stock (Fang et al. In preparation). This presumes that the buildings surveyed have high column loads relative to smaller building typologies.

In a related study, an office, hospital and school were designed using 8 different steel and concrete structural systems to compare the impact of program and material specification on upfront carbon. These buildings are of similar scale to those studied by Pratt and can be classified as medium rise buildings of regular geometry with no basement. The superstructure and substructure combined contributed over 50% of the building's total embodied carbon, with the substructure accounting for 11-17% (Kaethner and Burrige 2012). The average normalized embodied carbon of the foundation by gross floor area in Pratt's survey of existing buildings accounted for 170.3 kgCO_{2e}/m² (See Table 2) (Pratt 2016), while the normalized embodied carbon of the entire structural frame in Kaethner and Burrige's study was approximately 200 kgCO_{2e}/m² (Kaethner and Burrige 2012).

In both studies, the materiality of the superstructure did not substantially alter the total carbon emissions. Meaning that steel, composite and reinforced concrete frames resulted in similar emission values. However, as the foundation is resolving the loads from the building above, there is an opportunity to optimize the weight of the superstructure to reduce loads on the foundations, and in turn, reduce the embodied carbon of the overall system. In addition to foundations being materially intensive, this material is rarely recovered or recycled (see Fig. 04). For example, the steel rebar in foundations is irretrievable (Cooper and Gutowski 2017) but accounts for a significant portion of the foundations embodied carbon in a spread footing. Even in instances where a building is demolished above grade, the material that has been built below grade is rarely extracted or utilized.

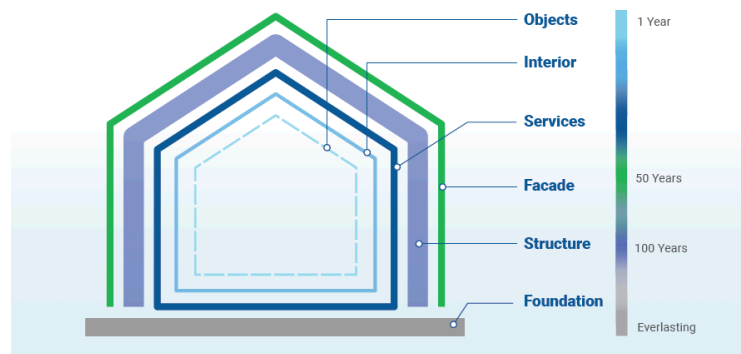


Figure 4: Typical Timeframe of Building Element Replacement (Adams, Burrows, and Richardson 2019)

1.3. OPPORTUNITIES

Reducing greenhouse gas emissions while meeting the demands of global urban growth is a design opportunity that calls for an abundance of performative and equitable design solutions. Foundations contribute a significant percentage of a building's overall embodied carbon. Optimizing their geometry to better distribute loads can reduce material consumption and carbon emissions substantially. Additionally, contemporary digital fabrication methods can be leveraged to construct more complex geometry in more contexts.

2. LITERATURE REVIEW

This chapter critically reviews current state-of-the-art in concrete structural design optimization, including foundation optimization, discusses prior applications of material efficient foundations and presents opportunities to construct them using digital fabrication.

2.1. CONCRETE STRUCTURAL DESIGN OPTIMIZATION

Since the second half of the 20th century, construction practices have trended toward simplicity at the expense of material efficiency. Typical shallow foundations work in bending, which is an inefficient method of load transfer. It requires that the foundations are large enough to spread the building load to the soil below, but are also thick enough in order to resist bending, meaning that more material is used than is required structurally. This is not dissimilar to other building systems which also typically work in bending, such as floor slabs and beams. In the Global North, this is typically done for ease of construction since labor costs outweigh material costs and it takes less time to build prismatic elements than those with complex geometry. However, by allocating material only where it is required structurally, there is an opportunity to help meet our climate goals by designing and building more efficient systems for the same floor area.

Three strategies of optimization typically explored for concrete structures are; size, shape and topology optimization. Size optimization can be described as interchanging materials (from reinforced concrete to mass timber, for example) to reduce environmental impact, where overall size of a structural element is prescribed. In this method, the mode of structural transfer is not changed when the element is optimized. However, there is potential for further savings by engaging with geometry. This could include a typology shift, for example from a flat concrete slab to a t-slab (See Fig. 5a), which would constitute shape optimization. However, further optimizing the geometry to allocate material only where it is required structurally, or topology optimization, unlocks additional savings (See Fig. 5b).

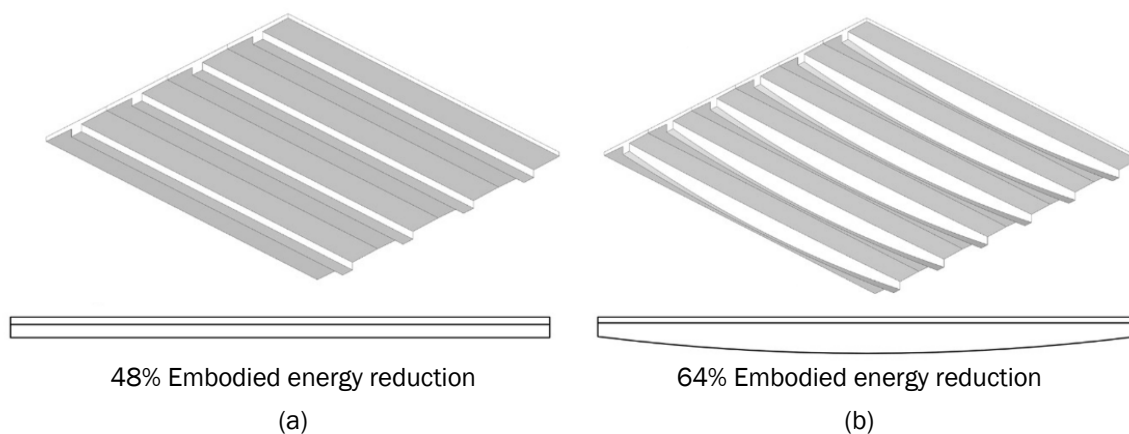


Figure 5: Embodied energy reduction from one-way reinforced flat concrete floor slabs through (a) shape optimization and (b) topology optimization, adapted from (Ismail and Mueller 2021)

Research by Ismail and Mueller shows that by optimizing the shape of a one-way reinforced concrete floor slab, embodied energy can be reduced up to 64% (accounting for both concrete and steel) (Ismail and Mueller 2021). Thin shell floors are also shown to reduce embodied carbon by 53-58% from an equivalent flat slab (Hawkins et al. 2020), while shape-optimized beams can save 40% of concrete compared to prismatic elements (Orr et al. 2011).

In a white paper by the Structural Engineering Institute’s Sustainability Committee Carbon Working Group, a modest saving of 10-25% was estimated as achievable through design optimization (“Achieving Net Zero Embodied Carbon in Structural Materials by 2050” 2020). However, these examples demonstrate that carbon savings well beyond 25% can be achieved by utilizing efficient geometry and computational design optimization. Yet, these methods have rarely been applied to foundations, presenting an opportunity to further reduce emissions in building structures.

2.1.1. FOUNDATION OPTIMIZATION

Concrete foundations are ubiquitous in global construction and have a high carbon impact. However, they are the structural element that is least studied through the lens of computational design optimization. In a survey of optimization articles for various reinforced concrete structural components, a total of 7 articles were found on foundations, compared to 152 articles for RC frame structures (Afzal et al. 2020). Of these 7 articles, not a single article was retrieved for the categories of material efficiency, and material efficiency and environmental performance (Fig. 6). Yet, foundations contribute between 10% and 40% of a building’s overall embodied energy (Pratt 2016) highlighting the fact that they are both highly impactful and highly understudied.

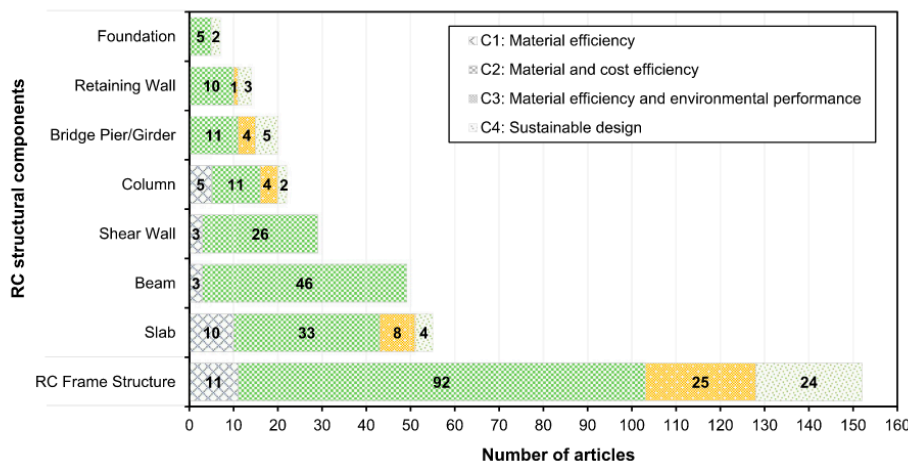


Figure 6: “Reinforced concrete structural components with number of collected articles in each [structural optimization] category” (Afzal et al. 2020)

To date, foundation design optimization has focused on small design spaces, looking at one or two design variables often related to cost (Camp and Assadollahi 2013) (Wang and Kulhawy 2008). Although insights are gained regarding the optimal shape of a spread footing for different contexts, marginal material savings are achieved. This is due to the fact that the optimization does not change the fundamental behavior of how the material is carrying the load, but is optimizing the height and depth within the confines of the existing spread footing topology.

Meanwhile there has been a lot of work on analog engineering of foundations that utilize efficient geometry to reduce material consumption. This presents an opportunity to combine the power of computational optimization with innovative geometry that can be built with digital fabrication. In order to reduce material consumption and embodied carbon in foundations, shell foundations are proposed to better utilize the material cross-section through membrane action, rather than bending. While it’s possible to use advanced numerical techniques such as topology optimization to generate the shell geometry, pure forms are used due to the extensive literature that’s been published on

their structural and geotechnical performance and their ability to save a significant percentage of overall embodied carbon.

2.2. EFFICIENT OR INNOVATIVE FOUNDATIONS THROUGH GEOMETRY

[Text from this section adapted from “Thin Shell Foundations: Historical Review and Future Opportunities (Feickert and Mueller 2021)]

By utilizing shells in foundations, a spatial system is created that distributes the applied loads primarily by in plane or membrane forces to the soil below, rather than through bending (Das 1989) (Williams 2014). Concrete is utilized most efficiently through direct compression. Therefore, if mainly compressive stresses are induced, a reduction in thickness and steel reinforcement can be achieved for the same applied load (Kurian 2006). By reducing material consumption, embodied carbon is ultimately reduced.

Historic examples suggest that material savings can be achieved by optimizing the geometry of foundations. Masonry arches can be considered the precursor to thin shell foundations, which have been utilized in India and other parts of the world dating back centuries (Fig. 7a) (Das 1989). For example, Christopher Wren designed inverted arch foundations for the Library for Trinity College, Cambridge, completed in 1695 (Fig. 7b) (Chiang, Buskermolen, and Borgart 2020).

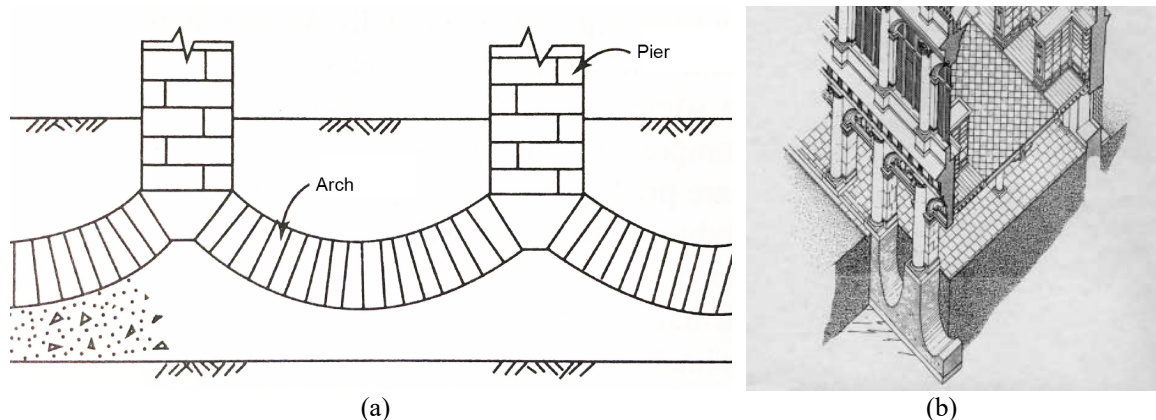


Figure 7: (a) Inverted arch foundations (Kurian 2006) (b) Library foundations, Trinity College (Chiang, Buskermolen, and Borgart 2020)

The first known example of a thin shell concrete foundation was constructed in 1953 by Félix Candela and Carlos Recamier for the Mexico City Customs House (Los Almacenes de las Aduanas) (Fig. 8) (Candela 1955). Candela utilized a combined linear arrangement of hyperbolic paraboloids (hypars), which derive their strength from their shape, rather than mass, as is typical in flat (spread) footings (Das 1989). A hyperbolic paraboloid is an anticlastic, doubly-curved surface which results in extraordinary strength to buckling (Candela 1955). Additionally, hypars are ruled surfaces, meaning the double-curvature can be formed with straight lines which has benefits from a construction perspective. If formwork is required, straight elements can be used rather than complex arched forms, reducing cost.

In the Mexico City Customs House project, the individual hypars measured 3.05m x 4.95m with a rise of 0.76m. The shells had a thickness of 152mm and were reinforced with 9.53mm bars at 203mm centers. In this example, there were no edge or ridge beams but 15.88mm diameter steel bars were located at the perimeter (Das 1989). Candela noted that the resulting cost was considerably lower than for a flat foundation supporting the same loads (Candela 1955).

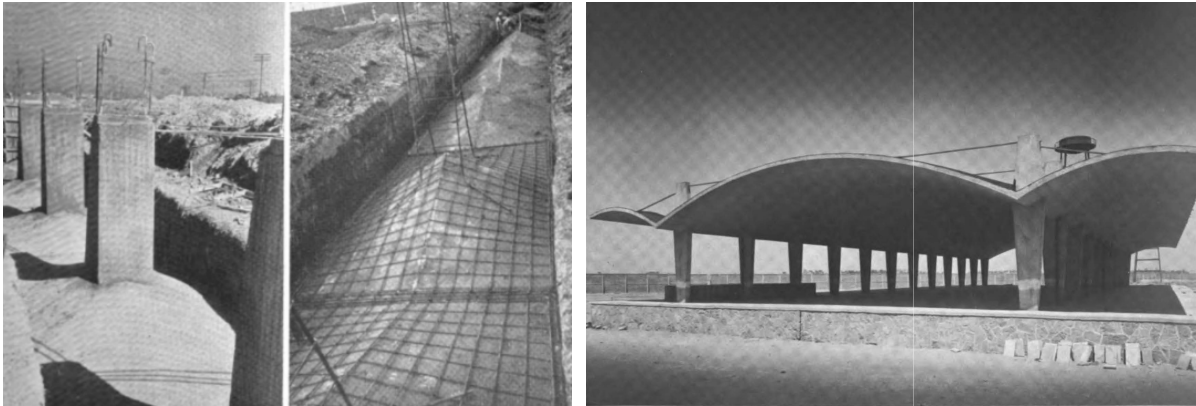


Figure 8: Shell footings for Mexico City Customs House, 1953 (Candela 1955) (Faber 1963)

The hyperbolic paraboloid is only one example of the various forms that shell foundations can take. Additional forms that have been studied in detail include shells of revolution such as cones and spherical domes, folded plates, cylindrical rafts and elliptic paraboloids (ellpars). As demonstrated in Figure 5, shells can either act as isolated footings or can be combined to form rafts depending on the shape of the footing and the configuration of the structural grid being supported, above.

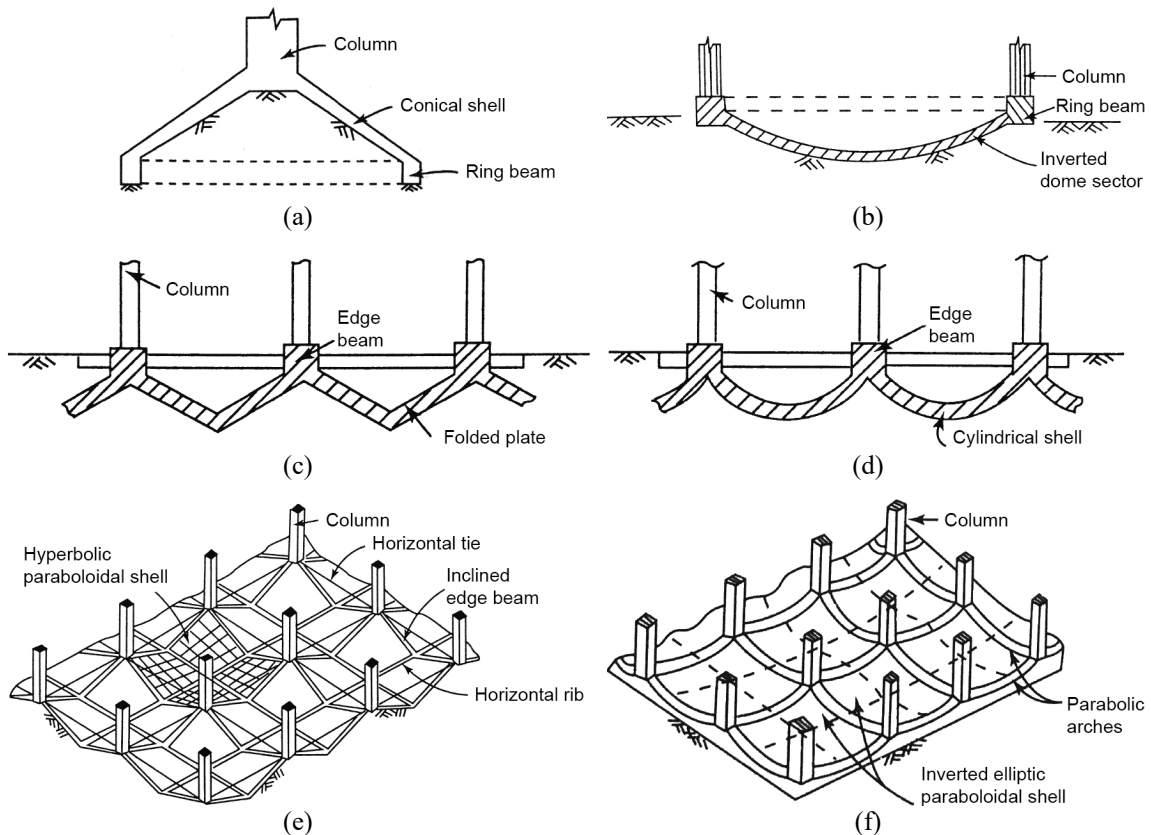


Figure 9: Various forms of shell foundations; (a) Conical, (b) Spherical dome, (c) Folded plate raft, (d) Cylindrical shell raft, (e) Hypar raft, (f) Ellpar raft (Kurian 2006) (text reformatted for legibility)

Other examples of thin-shell concrete foundations have been utilized in various parts of the world, namely Mexico, the former Soviet Union, Africa and India, however, their application has remained limited (Kurian 2006). Of the projects studied, the most significant cost savings was found to be 72% when a shell foundation was compared to a conventional raft foundation, and 55% compared to a pile foundation for a factory project in Konnagar, India. This project utilized an inverted continuous cylindrical shell foundation (similar to Fig. 9d) (Abdel-Rahman 1996).

The majority of built examples thus far utilize shells due to the opportunity to save cost by reducing material consumption. This is typical in contexts where material costs outweigh labor costs, predominantly in countries situated within the Global South. Shell foundations are therefore relatively understudied outside of this context. However, due to their ability to substantially reduce material consumption and, in turn, embodied carbon, these precedents provide motivation for revisiting shell foundations.

2.3. SHELL FOUNDATION ENGINEERING

[Text from this section adapted from “Thin Shell Foundations: Historical Review and Future Opportunities (Feickert and Mueller 2021)]

While Candela first experimented with shell footings in 1953, only a few decades after thin shell concrete roofs were formalized in Germany in the 1920s (Plunkett and Mueller 2015), the amount published on their application is extremely limited in comparison. Perhaps this can be attributed to the complexity that is added to the problem of shell design when the structure-soil interface is introduced.

2.3.1. SELECT CONTRIBUTORS TO SHELL FOUNDATION ENGINEERING

Despite their relatively infrequent use, significant literature on the theory and application of shell foundation engineering exists. At present, most research on shell foundations has been limited to India and Russia, although the largest number of built examples are located in Mexico (Kurian 2006). Contemporary research on shell foundations was first introduced to the author through the PhD thesis of Mohamed Abdel-Rahman (1996) of Concordia University, Quebec. Abdel-Rahman was advised by Professor Adel M. Hanna, and both have published considerably on the topic.

However, no author is as prolific as Nainan P. Kurian, who appears to have first published in the *Bulletin of the International Association for Shell and Spatial Structures* with Varghese in 1971. This was the same year he completed his PhD thesis in the Department of Civil Engineering at the Indian Institute of Technology (IIT), Madras (located in what is now Chennai). India is understood to be the only country with a building code devoted specifically to shell foundations (consisting of the conical and hyper types) which was drafted by Kurian (Kurian 2006). He is also the author of *Shell Foundations: Geometry, Analysis, Design and Construction* (2006) published by Alpha Science International Ltd. upon which much of this research is based.

It is interesting to note that Shri Puthenveetil Chandapillai (P.C.) Varghese, mentioned above, was the Head of the Department of Civil Engineering at IIT, Madras following his studies of soil mechanics at Harvard University beginning in 1948 (IIT Alumni). Varghese studied under Professors Karl Terzaghi and Arthur Casagrande who are considered to have established the discipline of soil mechanics together (ASCE). Excerpts of their work is summarized below.

2.3.2. SUMMARY OF PREVIOUS INVESTIGATIONS ON SHELL FOUNDATIONS

Foundation engineering must account for both structural design of the foundation and geotechnical design which includes an in depth understanding of soil mechanics. The primary function of the substructure is to sufficiently accept the loads applied by the superstructure and transfer them to the underlying soil without exceeding the allowable bearing stress or causing excessive settlement (Rinaldi 2012). Kurian notes that, “rigorous analytical solutions in closed form on the geotechnical performance of shell foundations – in terms of bearing capacity and settlement – are extremely complex to develop, due to the non-planar interface between the shell and the soil,” (Kurian 2006). This problem becomes even more complex when it is combined with the flexibility of the shell itself (Rinaldi 2012).

The strength by which shell foundations are designed depends on the distribution of the soil reaction pressure when a load is induced by the superstructure (Rinaldi 2012). Strength of a structural member manifests in its material and cross-section, and is therefore, directly relevant to the aim of reducing material consumption in structural design. However, there are limited examples in literature that study the contact pressure distribution under shell footings (Rinaldi 2012). This explains why shell foundations have typically been designed using membrane theory (Fig. 10d, 10e) with the addition of safety factors (Rinaldi 2012). Membrane theory assumes that the soil reactions are uniform if the applied load is concentric, or uniformly varying if the applied load is eccentric (Kurian 2006). It should be noted that conventional flat foundations are typically designed using membrane theory (Fig. 10a) although the pressure distribution is not uniform (Fig. 10b, 10c). However, flat foundations have been optimized to accommodate construction processes, rather than for material efficiency. Therefore, by understanding the structure-soil interaction in better detail, further material savings may be possible in shell foundation design.

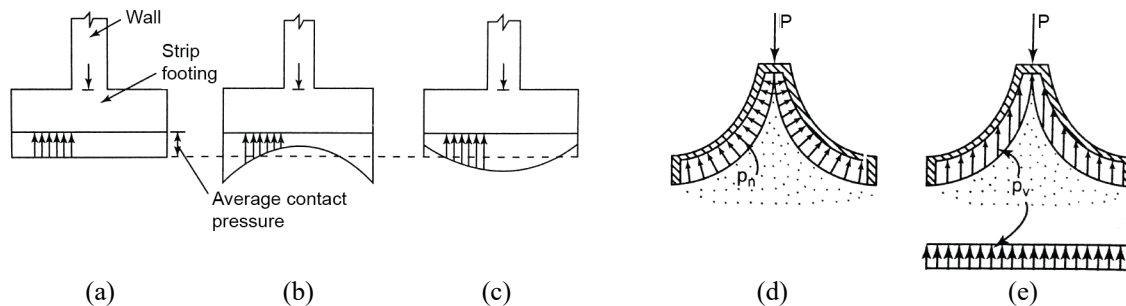







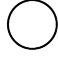

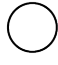

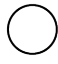

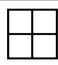

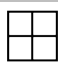






Figure 10: Pressure distributions; strip footing (a) rigid design (b) flexible design on cohesive soil (c) flexible design on cohesionless soil; shell footing (d) normal distribution (e) vertical distribution (Kurian 2006)

In order to better understand the response of soil under perfectly rigid shells, including bearing capacity and settlement, Kurian and Jayakrishna Devaki conducted an analytical investigation where they altered the geometry of the shell (Kurian 2006). They tested various pure shell forms with various ratios of the rise of the shell (f) to the length of half the base (a) (See Fig. 17b for dims). For the 44 configurations that were tested, the bearing capacity of the shell increased as the rise (f) increased as compared to the flat foundations for the same load in the upright configuration. The increase in bearing capacity ranges from 14-34% when the rise to half-base ratio (f/a) equals $1/2$ and ranges from 20-42% when the rise to half-base ratio equals 1. For inverted shells, bearing capacity decreases from 0-40% when (f/a) equals $-1/2$ and decreases from 10-60% when (f/a) equals -1 (Kurian 2006). An excerpt of these findings is shown in Table 3.

Table 3: Bearing capacity and settlement of shell foundations under axisymmetric 3-D analyses (Kurian 2006)

Type of footing	Section	Plan	Rise to half-base ratio (f/a)	Bearing capacity (kPA)	Settlement at 1/3 rd bearing capacity (mm)	Difference in bearing capacity from flat (%)
Flat square			0	148.14	0.450	0
Flat circular			0	103.04	0.171	0
Conical (upright)			+1/2	157.27	0.377	+34.47
Conical			+1	176.93	0.317	+41.75
Conical (inverted)			-1/2	73.60	0.308	+39.99
Conical			-1	73.60	0.384	-39.99
Hypar			+1/2	172.84	1.025	+14.28
Hypar			+1	185.19	0.552	+20.00
Hypar			-1/2	129.63	0.642	-12.49
Hypar			-1	98.77	1.453	-50.00

The investigation did not reveal consistent trends with respect to elastic settlements; however, bearing capacity was also found to increase with an increase in roughness at the interface between the soil and shell. It improved further with increased cohesion (c) and angle of internal friction (ϕ) of the soil (Kurian 2006).

Based on the historical applications and analytical and experimental findings, it can be summarized that shells offer an economical solution to distribute high column loads to weak soil while minimizing material consumption. Savings in carbon intensive concrete and reinforcing steel in fact increase when the column load applied increases and the allowable bearing pressure of the soil decreases. These savings are more sensitive to the bearing pressure. That is to say, as the bearing pressure decreases, shells become even more economical (Kurian 2006). Loads of up to 5 Meganewtons were evaluated for the hypar shell and up to 10 Meganewtons were evaluated for the conical shell. Additionally, shell foundations can have significantly improved bearing capacity (up to ~40%) compared to flat counterparts under the same load. By improving the structural performance of the foundation, significant material savings are possible.

2.4. OPPORTUNITIES FOR DIGITAL FABRICATION FOR SHELL FOUNDATIONS

[Text from this section adapted from “Thin Shell Foundations: Historical Review and Future Opportunities (Feickert and Mueller 2021)]

Innovations in digital fabrication have led to increased productivity and reduced cost for construction applications. These savings can be attributed to a machine's ability to fabricate complex designs in less time as well as the added potential to transfer fabrication data directly to full scale automated construction (García de Soto et al. 2018). For example, a mobile robot developed for on-site masonry construction is capable of laying up to 3 times more bricks than a human mason in the same amount of time (Sklar 2015). *The Sequential Roof* reduced construction time tenfold by implementing robust computational tools for design and automated construction (García de Soto et al. 2018). While these projects demonstrate the efficiencies of advanced manufacturing, few applications take advantage of using earth as a fabrication medium. Earth offers an opportunity for low cost and no waste formwork, providing motivation for highlighting work that has been done in this area thus far.

Earth as formwork is not a new concept, particularly in shell design and fabrication. Heinz Isler coined the term “freely shaped hill,” in his paper ‘New Shapes for Shells’ (1960) as a method for designing shells, where earth is formed into the desired shape and concrete is cast on top (Fig. 10a) (Moreyra Garlock and Billington 2014). In fact, Félix Candela used this same method for fabricating shell foundations in-situ in 1953 (Fig. 8), whereby soft clay was roughly cut into the approximate shape and then was refined by using a simple form, or template, which was coated with mortar (Candela 1955). Teshima Art Museum is a contemporary example of the same method at a much larger scale (Fig. 10b).



Figure 10: (a) Isler's freely shaped hill method (Gericke et al. 2016), (b) Earth formwork for the Teshima Art Museum (ArquitecturaViva)

These examples require skilled laborer's to manually prepare the earth to act as formwork. This is both time intensive and costly in contexts where labor costs outweigh material costs, which may explain why shell foundations have not seen widespread use. However, innovation in digital tools and advanced manufacturing has led to customized fabrication of complex geometry, while simultaneously reducing the material and labor required to build these systems. For example, additive manufacturing has received considerable attention for buildings, with 3D printed concrete being the most well-known application.

Advances in large scale 3D printing hardware and software have also been leveraged to 3D print earth at building scale. Utilizing locally available materials, Curth et al. 3D printed an earthen wall structure on-site with a mixture comprised of clay, silt, sand, chopped straw and water (Fig. 11a).

Mud mixtures can be formulated to achieve the same compressive strength as conventional mud bricks (Curth et al. 2020). However, the ratio of the individual materials crucially determines the ability to print the mixture and its capacity to withstand cracking and shrinkage (Curth et al. 2020) which are important considerations if earth is to be printed for formwork. Another full-scale prototype was 3D printed in earth in Valldaura natural park, Spain, which further demonstrates the possibility of printing complex geometry at building scale (Dubor, Cabay, and Chronis 2018). The material mix, composed of earth, water, fibers, sand and proteins was studied for its structural performance including shrinkage, brittleness, and the speed with which it cured. Non-uniform shrinkage and low compressive strength of the clay before it cured informed the toolpath and geometry which resulted in the conical diagrid structure, seen in Fig. 11b.



Figure 11: Full scale 3D printed earthen wall structures by (a) Curth et al. (image courtesy of Curth), and (b) Dubor et al. (IAAC)

Subtractive CNC milling for complex formwork is common practice, however these methods typically rely on carbon intensive materials such as high-density foam. Gericke et al. studied the possibility of freezing sand and CNC milling it to act as formwork for concrete elements (Gericke et al. 2016). The sand was able to be machined with high precision and remained intact during the concrete pour and curing. However, the milling process had to be optimised for specific time windows due to the uncontrolled environmental conditions that the frozen sand was subjected to during milling. This suggests that while sand can be utilised in subtractive manufacturing processes, alternative methods need to be developed for applications where limited control on climate is expected, specifically for heat stressed regions.



Figure 12: (a) “Feedback driven design explorations by students Ladina Ramming and Thorben Westerhuys” (b) HEAP autonomous walking excavator (Hurkxkens et al. 2020)

Topological interventions have been studied at building scale by Hurkxkens *et al.* (2020). By using the same end-effector but manipulating the toolpath, various earth formations have been created (Fig. 12a). The final formations were not tested for their ability to transfer structural loads; however, much can be learned from these experiments for load-bearing applications. Additionally, the use of an autonomous excavator has shown that shaping earth at scale is achievable (Fig. 12b). Subtractive methods have also been applied extensively in industry for applications such as car design and sculpture. Pure clay and casting sand maintain their shape when milled however, due to the complex nature of the interaction between the shell and the soil, these materials are not suitable for transferring structural loads in foundations.

2.5. RESEARCH GAP AND RESEARCH QUESTIONS

Materially efficient alternatives to existing building systems are necessary to explore in order to limit global warming while providing adequate housing for the increasing global population. The research questions that are central to this work are:

- To what extent can efficient geometry reduce carbon emissions in foundations?
- Can we leverage digital fabrication to construct complex geometry, if warranted by carbon savings?

To answer these questions, this thesis reviews the history of thin shell foundations (Sec. 2.2), quantifies the environmental impact of business-as-usual foundation design by deploying a computational workflow to design spread and shell footings (Sec. 4.1.1), evaluates the applicability of shell foundations to various building typologies and contexts based on their carbon saving potential (Sec. 4.1.2), quantifies the downstream global warming potential saving when multiple structural elements are optimized (Sec. 4.2), and investigates opportunities to construct shell footings using contemporary fabrication techniques (Sec. 5.2).

3. METHODOLOGY

In order to evaluate the environmental impact of shell foundations compared to prismatic (spread) foundations, the methodology in Fig. 13 is used.

3.1. COMPUTATIONAL DESIGN SPACE OF FOUNDATIONS

Existing physics-based analytical equations that design and size steel and concrete elements for shell and spread foundations are parameterized in a computational workflow. This allows one to quickly iterate through designs by varying the structural and geotechnical conditions (in the form of column loads and bearing capacities, respectively). Then, a series of studies is conducted by iterating through the parametric workflow in order to determine the applicability of shell foundations to various contexts and building typologies.

3.1.1. CONCEPTUAL OVERVIEW

Equations to design and dimension structural elements including foundations are well established in many codes and textbooks. They are typically executed manually for prescribed column loads and soil types for site specific applications. Alternatively, over-engineered solutions are deployed in contexts where site specific stratigraphy is not available or expensive to procure. This methodology parameterizes structural codes, material properties and geometric constraints for designing foundations for two reasons; 1) to understand the concrete and steel reinforcement material takeoffs of a given design in order to calculate the resulting embodied carbon, and 2) to quickly iterate through various structural and geotechnical conditions to output generalized data to understand the applicability of shell and spread footings to various contexts.

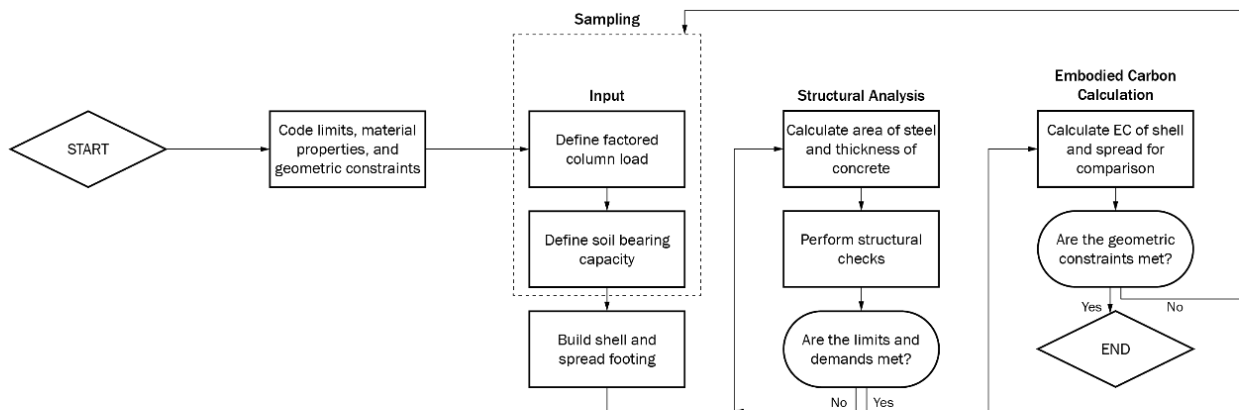


Figure 13: Methodology for structural design and embodied carbon comparison of spread and shell footings

Due to the fact that the only known building code for shell foundations is from India, this thesis references the National Building Code (NBC) of India for structural mechanics, specifically the Indian Standard 456-2000: Plain and Reinforced Concrete Code of Practice (IS 456) (Bureau of Indian Standards 2000). This code can be compared to American Concrete Institute Code 318-19 (Building Code Requirements for Structural Concrete and Commentary), but is more conservative in some regards (Ismail and Mueller 2021).

Limits imposed by the National Building Code, material properties and geometric constraints are coded into a parametric workflow to design shell and spread footings (See Table 4). While all inputs

are parameterized, the variables that were changed for this study were the factored column load and the soil bearing capacity. The factored column load is a result of the design of the building above grade. The size, materiality and program of the building all have substantial impact on the forces being resolved by the foundations and their resulting size. Similarly, foundation design depends on the stratigraphy of the site and the resulting bearing capacity of the soil which typically ranges from 72kN/m² for clay soil to 575kN/m² for bedrock. Soil types are well distributed throughout the world, with the U.S. shown in Figure 14 (Horton, Carma, and Stoeser 2017). This research studies how changes in the factored column load and soil bearing capacity impact the overall carbon emissions of the system.

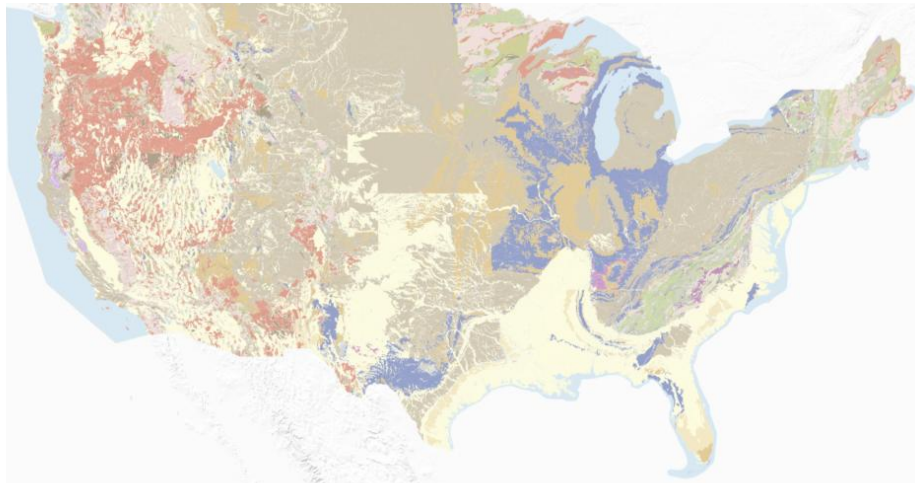


Figure 14: State Geologic Map Compilation of the conterminous United States (Horton, Carma, and Stoeser 2017)

Once these variables are chosen, the workflow calculates the area of steel and the thickness of concrete for the respective designs. It performs the required structural checks by code and determines if those limits are met. If yes, the material quantities are extracted in order to calculate embodied carbon. The inputs are then iterated through in order to create generalized data to understand how each design performs under different conditions.

This research focuses specifically on the embodied carbon impact of shallow foundations as they require less material than deep foundations, where applicable. This is due to the fact that the same end-bearing area is required, for deep foundations, at depth. This simplification does not account for friction piles, which were beyond the scope of these experiments.

Table 4: Material properties for structural design and embodied carbon calculation *Values from ICE database 2019 (Hammond and Jones 2008)

Material	Embodied Carbon Coefficient* (kgCO _{2e} /kg)	Density (kg/m ³)	Strength, σ (MPa)	$x_{u\ max}/d$
Plain concrete	0.15	2323	23	-
Steel, Rebar	1.99	7849	415	0.456

The workflow assumes that a column transfers the load of the building to an aligned footing, located in the center of a tributary area of 84m². The geometry of the foundation is constrained by the

tributary area so as to prevent overlap as the structural grid expands. It should be noted that in typical foundation design, when the area of individual spread footings exceeds 50% of the building footprint, a typological shift typically occurs and mat foundations replace individual footings. However, in this research, the minimum material required to support the design load is being calculated until the geometric constraint is reached. This means that the embodied carbon values shown are likely less than the values that would result from current construction processes.

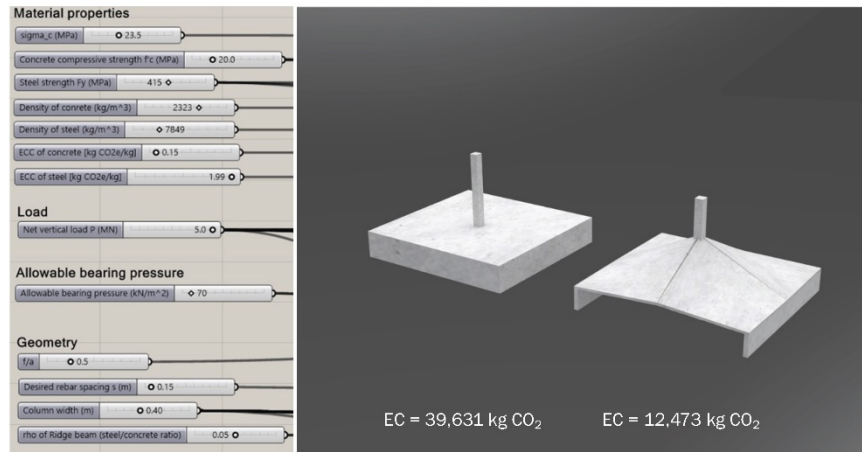


Figure 15: Inputs for parametric workflow and resulting design and embodied carbon for spread and shell foundations

The resulting structural design and embodied carbon values for a set of inputs in the parametric workflow are shown in Figure 15.

3.1.2. STRUCTURAL DESIGN OF SPREAD FOOTINGS

The structural design for spread footings follows the design procedures outlined in *Design of Foundation Systems* (Sec. 8.2) (Kurian 2004). The key dimensions are described by Figure 16a and the section is shown in Figure 16b.

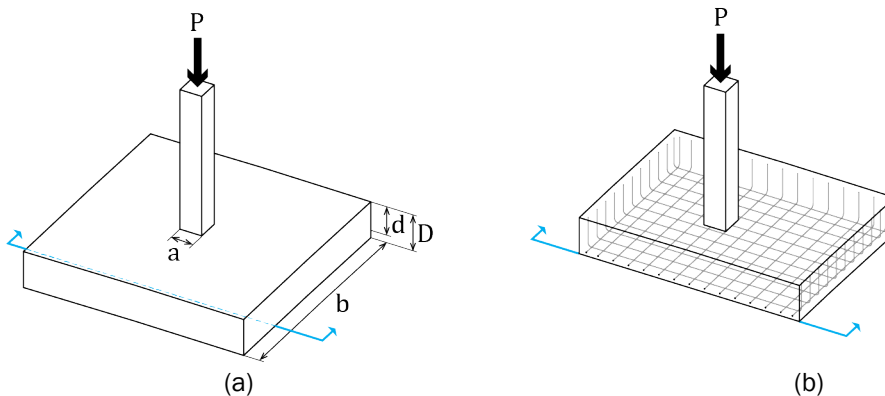


Figure 16: (a) Dimensions of spread footing, and (b) section of spread footing

In order to calculate the area of steel and thickness of concrete for the shell, the column load, P , is first multiplied by a factor to safety (1.5) to get the factored design load, P_u . After calculating the design punching shear strength, τ_c , using Eq. (1), the depth of the footing, d , is calculated by setting

the total shear force on the critical section equal to the total resistance of the section in punching shear (Eq. 2).

$$\tau_c = 0.25\sqrt{f'_c} \quad (1)$$

$$P_u[b^2 - (a + d)^2] = 4\tau_c(a + d)d \quad (2)$$

Next, the ultimate bending limit, M_u , is calculated using Eq. (3). This value is then set equal to Eq. (4) to find the depth, d , for bending moment.

$$M_u = (P_u/2)((b - a)/2)^2 \quad (3)$$

$$M_u = [0.36\left(\frac{x_{u\max}}{d}\right)\left(1 - 0.42\frac{x_{u\max}}{d}\right)f'_c]bd^2 \quad (4)$$

The higher value is taken from the depths calculated for punching shear, d_{ps} , and bending moment, d_{bm} , to design the area of steel, A_s . The depth for punching shear is typically greater than the depth for bending moment. In either case, the area of steel, A_s , can be calculated using Eq. (5).

$$M_u = 0.87\sigma_{st}A_s d \left(1 - \frac{A_s\sigma_{st}}{bdf'_c}\right) \quad (5)$$

$$P_u[b^2 - (a + d)^2] = 4\tau_c(a + d)d \quad (6)$$

A rebar diameter is selected, ϕ , and Eq. (7) is used to calculate development length. Design bond strength, τ_{bd} , is prescribed by Cl. 26.2.1.1 in the Code (Bureau of Indian Standards 2000) and is multiplied by 1.6 for deformed bars in tension. The length of rebar is then checked to make sure it satisfies the development length using straight bars and subtracting for concrete cover, cov , using Eq. (8).

$$L_d = \phi\sigma_{st}/4 * 1.6\tau_{bd} \quad (7)$$

$$L_d > \left(\frac{b - a}{2}\right) - cov \quad (8)$$

The percentage area of steel is checked against a minimum of 12% [C1:Cl.26.5.2.1] and then the section is checked to make sure it is over-reinforced using Eq. (9).

$$\frac{0.87\sigma_{st}A_s}{0.36f'_c bd} < \frac{x_{u\max}}{d} \quad (9)$$

Depth is then determined for bending shear, d_{bs} , using Eq. (10), where the design strength of concrete, τ_c , is prescribed by Code (Table 19, IS 456:2000).

$$d_{bs} = (P_u(b - \frac{a + 2d}{2}))/\tau_c \quad (10)$$

Lastly depth calculated for bending shear, d_{bs} , is checked to ensure it is less than the maximum depth obtained from Eq. 2 and Eq. 4. If the depth for bending shear is greater than the depth from Eqs. 2 and 4, the depth must be revised to satisfy bending shear.

For this study, within the geometric constraints of the spread footing, the two structural checks that are not always met are; 1) that the development length of the rebar is greater than the width of the

footing minus sufficient cover, and 2) that the section is under reinforced. When a reinforced concrete element is under reinforced, there is danger that the failure will occur in the concrete section, rather than in the steel. This is dangerous as concrete experiences a sudden, brittle failure, giving no warning to occupants, as opposed to steel failure, which occurs slowly. For the development length, the initial design assumes that rebar remains straight and is not turned up at the edge, due to the added complexity of maintaining it in position while concrete is poured. However, if sufficient development length is not achieved, it is assumed that the bars will be bent or hooked in order to achieve sufficient length. This occurs only within a small number of combinations, at low applied loads (0-1MN). In order to address under reinforcement, thickness is added incrementally until all structural checks are satisfied for the given load case.

In parallel, a hyperbolic paraboloid (hypar) shell footing is designed for the same inputs as the spread footing.

3.1.3. STRUCTURAL DESIGN OF SHELL FOOTINGS

The structural design for a hypar shell footing is completed following design procedures outlined in Kurian's textbook, *Shell Foundations: Geometry, Analysis, Design and Construction* (Sec. 6.4.2) (Kurian 2006). The shell membrane, edge beams and ridge beams are designed for simplified load cases. Uniform thicknesses are maintained, in line with Kurian's example, to be conservative. The rebar is designed to follow the lines of tension as the quantity of steel can be reduced by half, when compared to designing rebar to follow the straight-line generators (Kurian 2006). The key dimensions and forces are described by Figures 17a and 17b.

Hyperbolic paraboloid shells are investigated due to their geometry. They are comprised of doubly curved, anticlastic quadrants that can be constructed using straight line generators in either direction. This means hypars are both stiff and more easily fabricated than other shell typologies as the reinforcing steel can be straight. They have also been deployed in applications throughout the world, as demonstrated by Félix Candela's examples in Mexico (See Sec. 2.2).

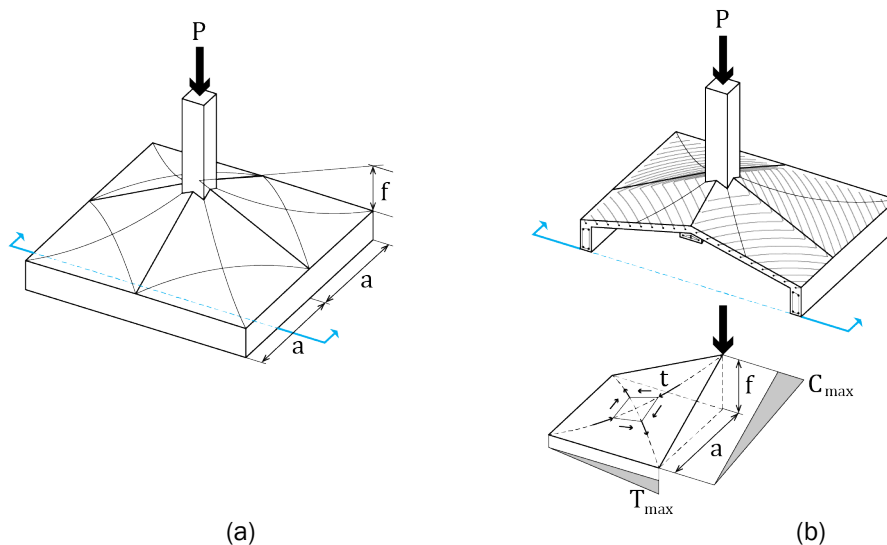


Figure 17: (a) Dimensions of shell footing, and (b) section of shell footing with forces

In order to calculate the area of steel and thickness of concrete for the shell, the column load, P , is first multiplied by a factor to safety (1.5) to get the factored design load, P_u . The membrane shear, t ,

is a function of the geometry of the shell. For a hyperbolic paraboloid, the warp, k , is calculated using Eq. (11), and the membrane shear is then calculated using Eq. (12).

$$k = f/a^2 \quad (11)$$

$$t = P_u/2k \quad (12)$$

To calculate area of steel by strength, a safety factor (0.87) and the following Eq. is used:

$$A_s = t/(0.87\sigma_{st}) \quad (13)$$

The thickness of the shell, h , can then be calculated using:

$$m = 280/(3\sigma_c) \quad (14)$$

$$h = (t/1.5)/(0.14f'_c - (m - 1)A_s) \quad (15)$$

Once the concrete thickness h is calculated, it is checked against a minimum thickness. If $h < 120mm$, 120mm is used, as prescribed by Code. The percentage area of steel is checked against a minimum of 0.5% and then the compressive stress in concrete ignoring steel is checked against the compressive stress in the equivalent section in the perpendicular direction using:

$$(t/1.5)/120 < (0.4f'_c)/1.5 \quad (16)$$

The area of steel in the edge beam is calculated to satisfy the maximum tension (located at the center of the beam) using Eq. 17. The height and width of the edge beam can then be found using Eq. 18.

$$A_{seb} = 2t/(0.87\sigma_{st}) \quad (17)$$

$$h_{eb} = \sqrt{(2t/1.5)/(m - (m - 1)A_{seb})} \quad (18)$$

Geometry of the ridge beam is designed following the steps outlined in Section 6.4 (Kurian 2006). Some geometric parameters are variable, such as the column width and rebar spacing, and are included as inputs into the parametric workflow. The values used for the following experiments are outlined in Table 5.

Table 5: Geometric and material properties for ridge beam calculations (Kurian 2006)

Steel to concrete ratio, γ	Column width, c (m)	Rebar spacing, (m)
0.05	0.4	0.15

The area of concrete in the ridge beam is calculated using Eq. (19), and the area of steel in the ridge beam is calculated using Eq. (20).

$$A_{crb} = (2t * \sqrt{(a^2 + f^2)})/(0.4f'_c - \rho_s * 0.4f'_c + \rho_s * 0.67\sigma_{st}) \quad (19)$$

$$A_{srb} = A_{crb} * \gamma \quad (20)$$

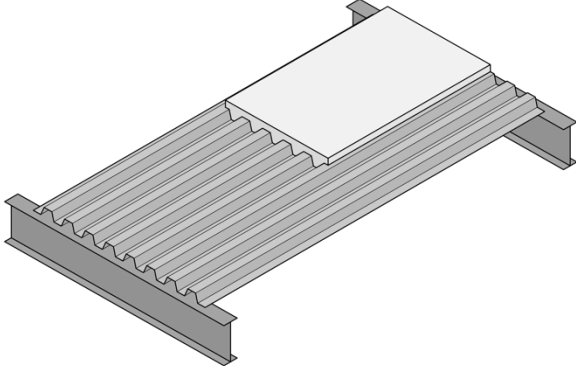

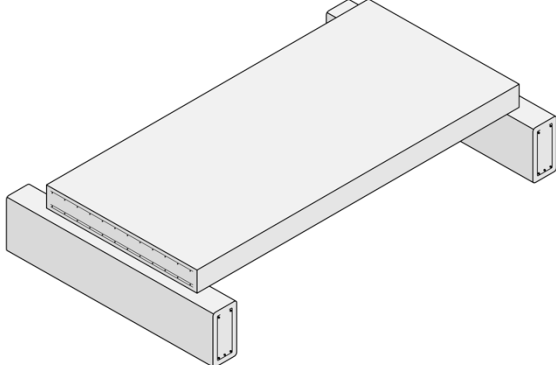
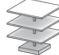
3.1.4. EMBODIED CARBON CALCULATION

The resulting structural designs from Sections 3.1.2 and 3.1.3 are then used to calculate embodied carbon using the material properties in Table 4. The volume, V , of concrete and steel, respectively, are extracted from the workflow and multiplied by their density, ρ , and embodied carbon coefficient, ECC , to determine the total kg CO_{2e} for each of the elements (Eq. 21). It should be noted that the volume of steel is not subtracted from the volume of concrete, as the difference is deemed negligible for the following experiments.

$$\text{Embodied carbon} = V * \rho * ECC \quad (21)$$

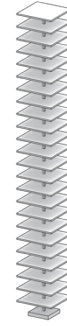
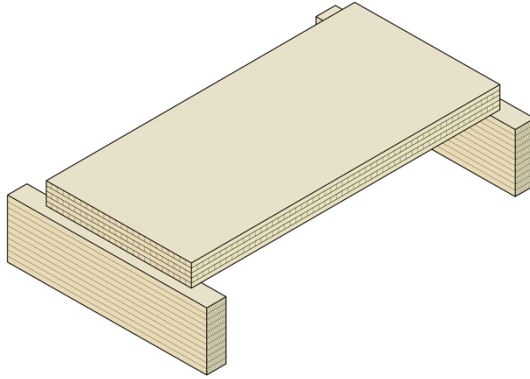
To assess the environmental impact of the materiality of a buildings structural system on foundations, three floor systems are studied. The deadload of a composite steel deck and concrete slab system, a concrete flat slab, and cross-laminated timber (CLT) slab is estimated in Table 6. The number of floors achieved that exert 2MN of force on the foundations is also noted in Table 6 in order to normalize carbon emissions by floor area for the respective systems.

Table 6: Floor build-ups and equivalent number of floors for a 2MN column load

Floor build-up:		# Floors for 2MN
Steel deck + concrete slab P ~ 90 lb/ft ² ~ 440 kg/m ²		 6
Concrete flat slab P ~ 180 lb/ft ² ~ 880 kg/m ²		 3

**Cross-laminated
timber (CLT) slab**

P ~ 20 lb/ft²
~ 100 kg/m²



24

3.2. WHOLE BUILDING FRAME ANALYSIS

The parametric workflow described in Section 3.1 is then linked to a larger full building structural model, that computes dimensions for structural members and incorporates optimization packages from fellow Digital Structures researchers. The purpose of this study is to understand how shape-optimized structural elements can be used in combination in order to reduce the overall global warming potential of a structural frame during the design stage of a project. The model is flexible and parametric, allowing designers to vary a range of inputs.

For this study, the full building model is calibrated using the values in Table 7. Any reductions or increases in global warming potential are measured against this baseline to determine how the optimization of structural elements can impact cumulative GWP of a structural frame.

Table 7: Values used for calibrating the GWP of the whole building frame analysis

Building Length	Building Width	Building Height	Floor-to-floor Height	Concrete Strength	Soil Bearing Capacity	ECC (kgCO ₂ e/kg)
50m	30m	24m	4.0m	40MPa	72kN/m ²	0.2768

Since foundations are furthest downstream in a buildings load path, their size can be reduced if the weight of structural elements upstream is reduced. By shape-optimizing floors, for example, a significant reduction to the column load being resolved by the foundations results in a reduction in overall embodied carbon. Factored column loads, P_u , are extracted from the larger building frame model and are used as inputs for the parametric workflow described in Section 3.1. Shape-optimized floor slabs are incorporated from, *Minimizing Embodied Energy of Reinforced Concrete Floor Systems in Developing Countries through Shape Optimization*, (Ismail and Mueller 2021) and different combinations of shape-optimized floors and foundations are studied to understand their interaction and emissions reduction potential (Section 4.2.1).

A study to evaluate the impact of concrete strength and shape-optimization of structural elements on embodied carbon is also conducted (Section 4.2.2). For this study, a range of embodied carbon coefficients are used, as emissions vary with concrete strength. A linear regression is used to approximate the embodied carbon coefficients of concrete based on strength for the self-reported Environmental Product Declarations for concrete in Mexico in the EC3 database (See Table 8) (EC3).

Table 8: Embodied carbon coefficient based on concrete strength for Mexico City

Concrete Strength	Embodied Carbon Coefficient
20 MPa	0.1808
30 MPa	0.2288
40 MPa	0.2768
50 MPa	0.3248
60 MPa	0.3728

4. EXPERIMENTS / RESULTS

The following experiments utilize the parametric workflow outlined in Section 3 to size steel and concrete in foundations to determine a shells ability to save embodied carbon through efficient geometry.

4.1. SINGLE ELEMENT COMPARISONS

The design of foundations is highly specific to the load being imposed by the building above and the underlying soil strata. Various combinations are highlighted below.

4.1.1. EMBODIED CARBON COMPARISON OF SPREAD FOOTINGS VERSUS SHELL FOOTINGS

Focusing first on low bearing capacity soil ($q=72\text{kN/m}^2$), hyperbolic paraboloid shells save a significant amount of embodied carbon when compared to a spread footing. For a 2MN load (See Table 6), the shell saves 48% CO_{2e} of the spread foundation for the same applied column load and soil bearing capacity (4,122 kg CO_{2e} and 8,001 kg CO_{2e}, respectively) (See Fig. 18). As the applied column load increases, the performance also increases. For a 5MN load, the shell saves 63% of the carbon emissions of the spread footing (12,319 kg CO_{2e} and 32,887 kg CO_{2e}, respectively) (See Fig. 18). The footings reach the geometric constraint of their tributary area at a column load ~5MN in clay soils, ending the iterative design process for both typologies.

As the bearing capacity increases from clay to sand, shells continue to outperform spread footings, although the extent of their savings is slightly reduced. For a 2MN load, the shell footing saves 39% CO_{2e} of the spread footing (3,612 kg CO_{2e} and 5,945 kg CO_{2e}, respectively) (See Fig. 19). For a 5MN load, the shell saves 56% of the carbon emissions of the spread footing (10,807 kg CO_{2e} and 24,502 kg CO_{2e}, respectively) (See Fig. 19). Although the extent of the savings are reduced from clay soils, they are still substantial and warrant exploration to determine how to construct them.

This study is extended to all soil types in Experiment 4.1.2.

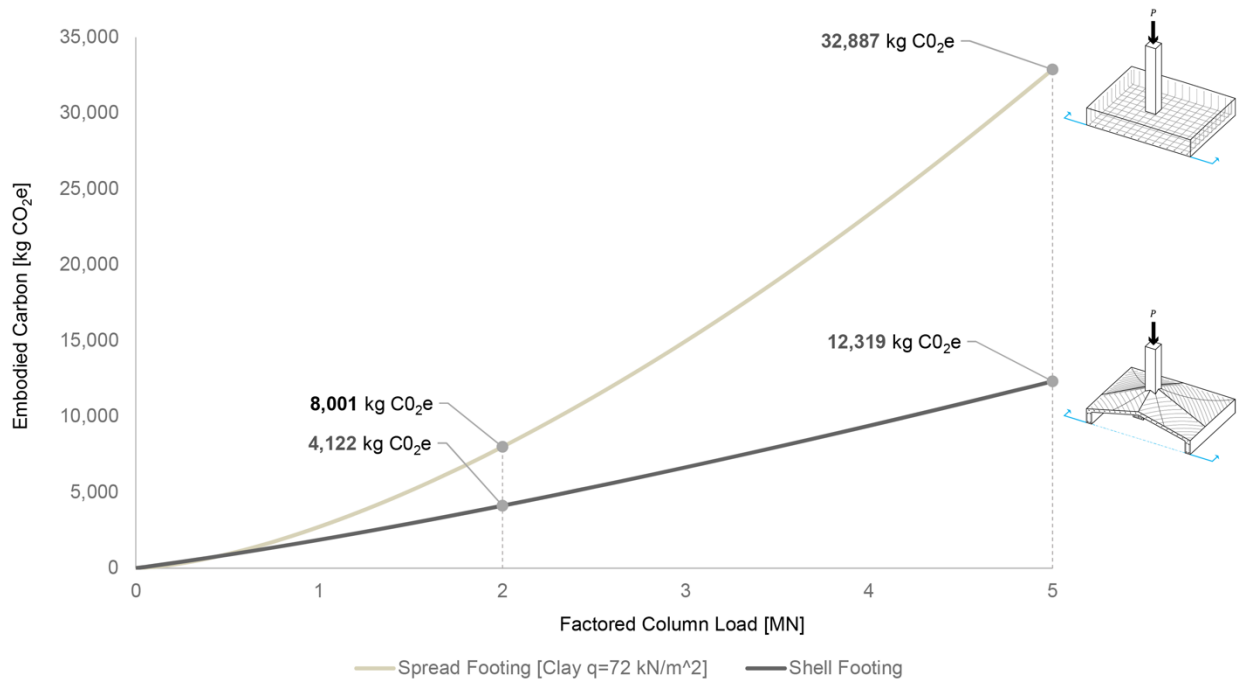


Figure 18: Embodied carbon for spread and shell footing on clay soil

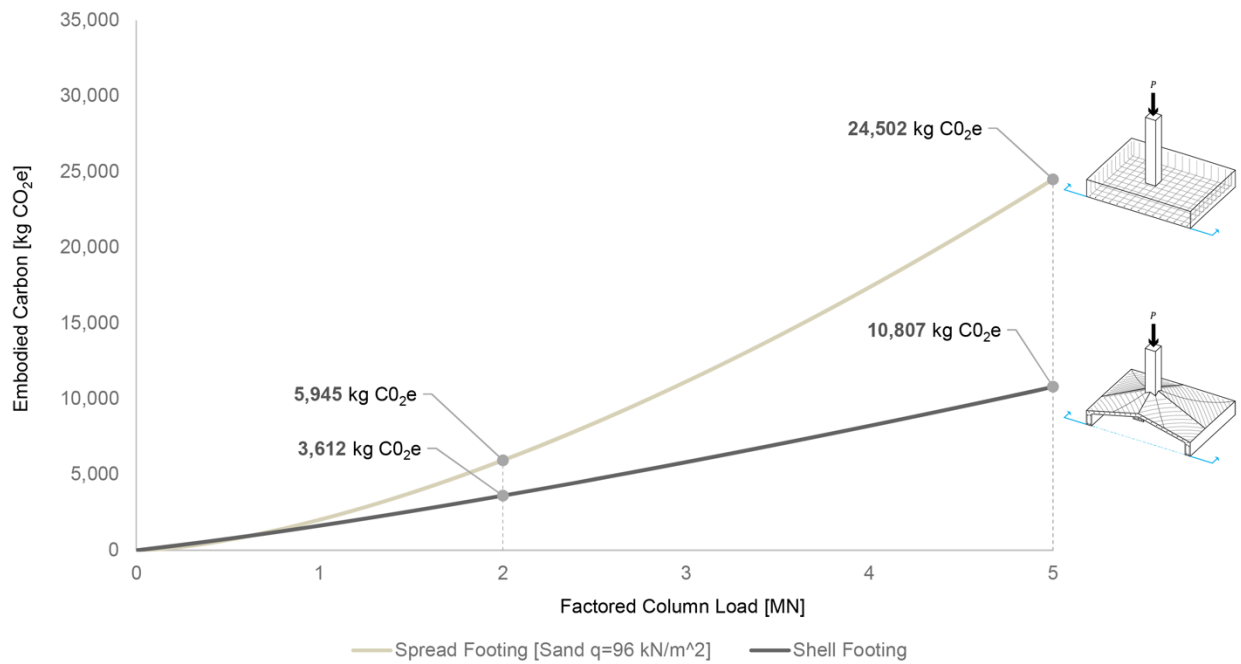


Figure 19: Embodied carbon for spread and shell footing on sandy soil

4.1.2. APPLICABILITY OF SHELLS TO VARIOUS CONTEXTS

Bearing capacities ranging from clay ($q=72\text{kN/m}^2$) to bedrock ($q=575\text{kN/m}^2$) and building loads ranging from 1MN to 5MN are iterated through to create generalized data for the total embodied carbon of both a spread footing (Fig. 20) and a shell footing (Fig. 21). This study allows one to compare the relative environmental performance of the same foundation typology for a given column load and soil type.

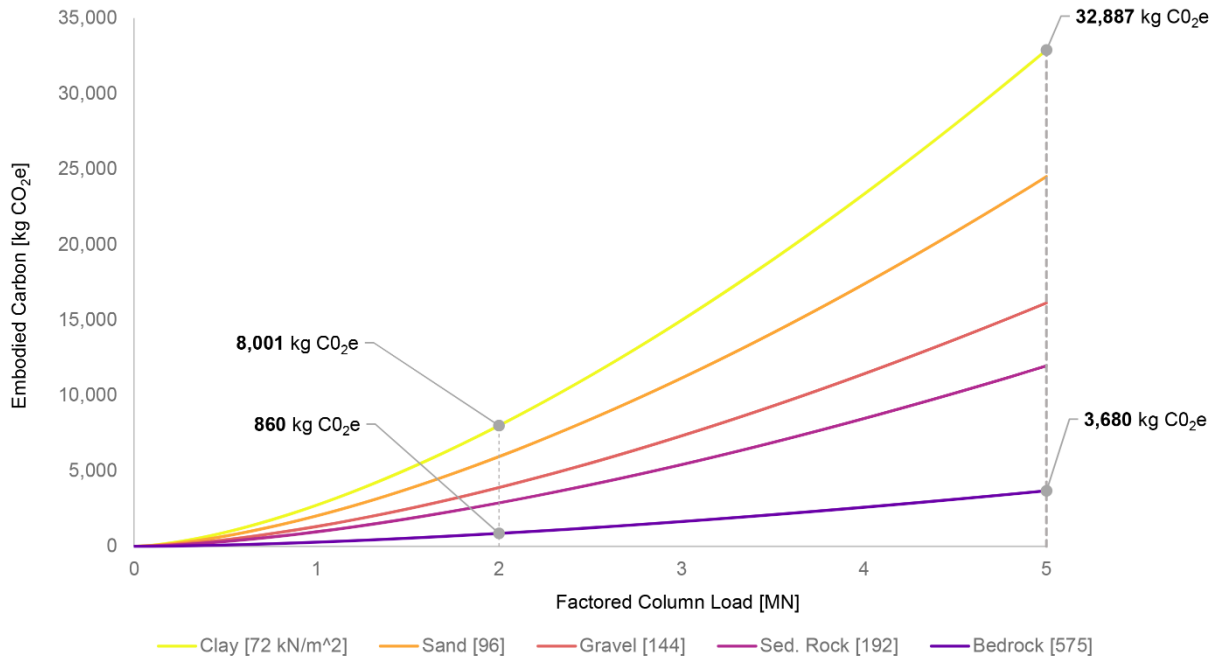


Figure 20: Impact of soil bearing capacity and column load on embodied carbon for spread footings

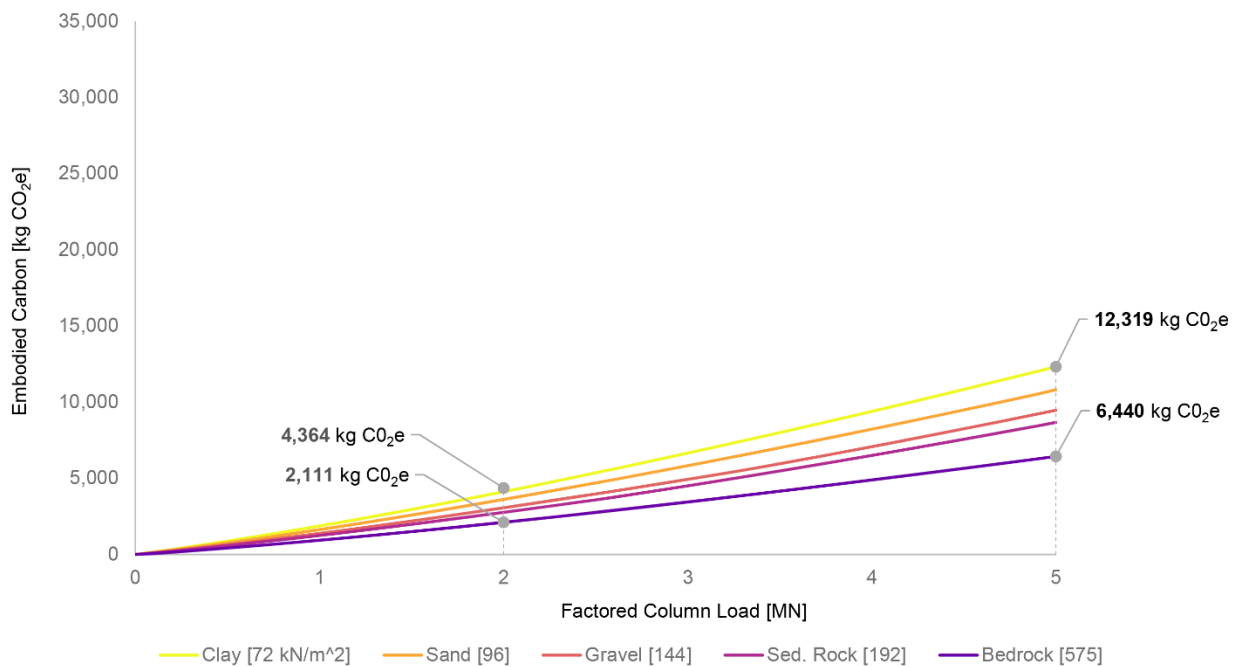


Figure 21: Impact of soil bearing capacity and column load on embodied carbon for shell footings

For the spread footing, a large range of embodied carbon values can be seen (Fig. 20). This is due to the fact that spread footings require that the area of the foundation is large enough to spread the load of the building to the soil below, but also that they are sufficiently thick to resist bending, which is an inefficient method of load transfer. As the column load increases in low bearing capacity soil, the amount of material required to resist bending increases substantially, accounting for 32,887 kg CO_{2e} for a 5MN column load. Therefore, spread footings are particularly inefficient for this application.

The design space for shell footings is much flatter than spread footings, meaning they perform similarly in a range of soil types (Fig. 21). This makes their performance particularly advantageous in low bearing capacity soils (sand, clay, gravel), as opposed to the spread footing, which requires a significant amount of material and results in large quantities of carbon. However, for high bearing capacity soils (bedrock), shells do not outperform their prismatic counterparts (See Tables 9, 10). This is explored in more detail in Figure 22.

Table 9: Total embodied carbon for spread and shell footings in various soils for 2MN load

Foundation Typology	Total EC, Clay (kgCO _{2e})	Total EC, Sand (kgCO _{2e})	Total EC, Gravel (kgCO _{2e})	Total EC, Sed. Rock (kgCO _{2e})	Total EC, Bedrock (kgCO _{2e})
Spread	8,001	5,945	3,896	2,876	860
Shell	4,122	3,612	3,062	2,762	2111
% saving of shell over spread	-48%	-39%	-21%	-4%	+46%

Table 10: Total embodied carbon for spread and shell footings in various soils for 5MN load

Foundation Typology	Total EC, Clay (kgCO _{2e})	Total EC, Sand (kgCO _{2e})	Total EC, Gravel (kgCO _{2e})	Total EC, Sed. Rock (kgCO _{2e})	Total EC, Bedrock (kgCO _{2e})
Spread	32,887	24,502	16,134	11,961	3,680
Shell	12,319	10,807	9,468	8,666	6,440
% saving of shell over spread	-63%	-56%	-41%	-28%	+75%

In order to compare the performance of the two typologies, the design space is visualized in 3 dimensions (See Fig. 22). Column load is shown on the x-axis [MN], soil bearing capacity is shown on the y-axis [kN/m²], with the resulting embodied carbon shown on the z-axis [kg CO_{2e}]. It should be noted that this visualization represents the range of soil types that are present, not their prevalence. For example, it's rare to see bedrock present at the surface of site stratigraphy and is more common to see lower bearing capacity soils such as clay, sand and gravel. Therefore, one should focus on the embodied carbon saving potential of these lower bearing capacity soils due to the potential application of shells in these contexts.

The significant savings that shells achieve for low bearing capacity soils and high applied column loads are prominent in Figure 22. However, shells do not always outperform spread footings, which is indicated by the gray surface being located above the tan surface.

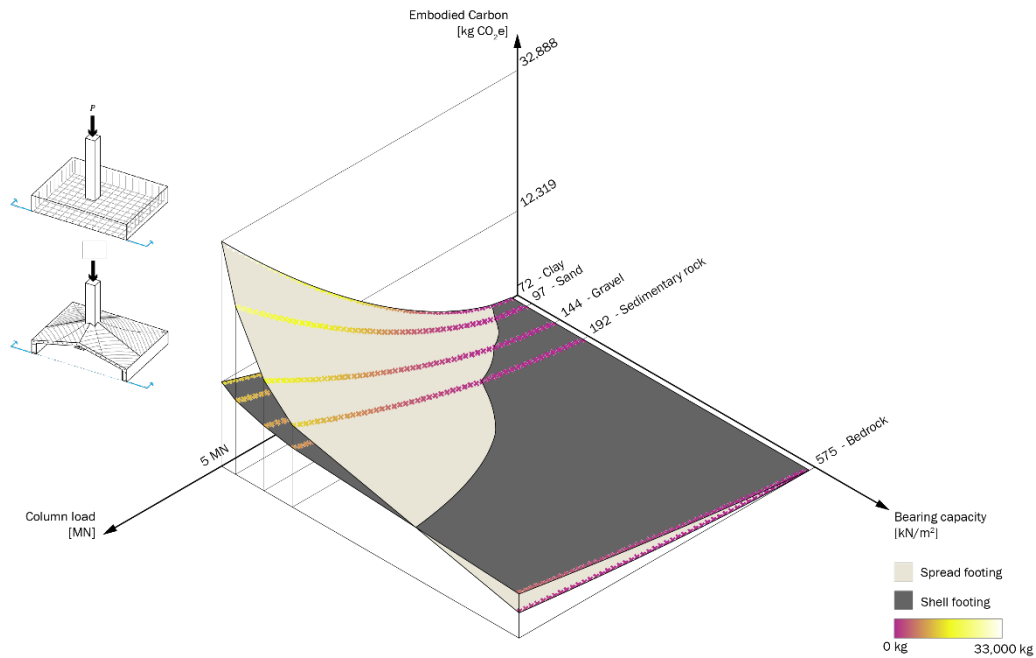


Figure 22: Total EC contribution for spread and shell footings resulting from soil bearing capacity and column load

This is attributed to two findings; 1) that the minimum concrete cover for reinforcement in shells results in a thickness much greater than the thickness required to satisfy the structural loads, and 2) the added curvature of the shell for a small footprint increases total material quantities. To satisfy the structural design code, the minimum shell thickness is set at 120mm to provide sufficient thickness for cover. In theory, however, the shell could be infinitely thin.

This suggests that alternative reinforcement can be explored, such as fabric, to reduce the thickness and total embodied carbon by removing steel in the shell surface entirely. Another opportunity to reduce embodied carbon in the shell is to optimize the edge beam and ridge beam, which are currently designed as prismatic elements. As the tension of the edge beam is highest in the center of the shell edge and reduces to zero at the corner, the shape could be optimized to reflect this. Reinforcement continuity would be a challenge in this study, but warrants further exploration. Similarly, the highest compressive force is located at the interface of the shell with the column, therefore, the ridge beam could be reduced to zero and the load is distributed into the shell membrane.

The environmental impact of concrete (Fig. 23) and steel (Fig. 24) to total embodied carbon is extracted from the study above to determine their respective contribution to the overall design. The total embodied carbon of both the shell and the spread footing comes almost entirely from concrete. This explains why the surfaces in Figure 23 are very similar to those of Figure 22. The quantity of concrete is more sensitive to applied loads than to bearing capacity, with the highest divergence between the shell and spread footing occurring at low bearing capacity soils. As the bearing capacity of the soil increases, the difference in concrete volumes and GWP between the shell and spread footing decreases significantly.

The volume of steel contributes much less to the overall embodied carbon of foundations than concrete (Fig. 24). In contrast to concrete, steel is more sensitive to the bearing capacity than to the applied load. For low bearing capacity soils, steel volumes are more comparable for spread and shell

footings. However, as the bearing capacity of the soil increases, shells require significantly more steel than spread footings.

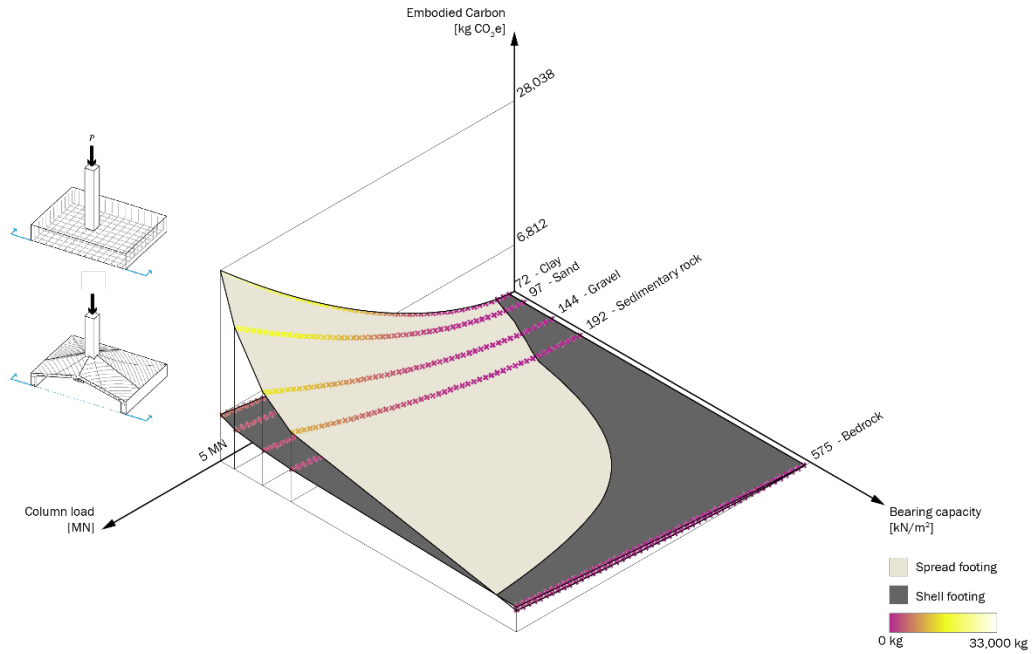


Figure 23: Partial EC contribution from concrete for spread and shell footings resulting from soil bearing capacity and column load

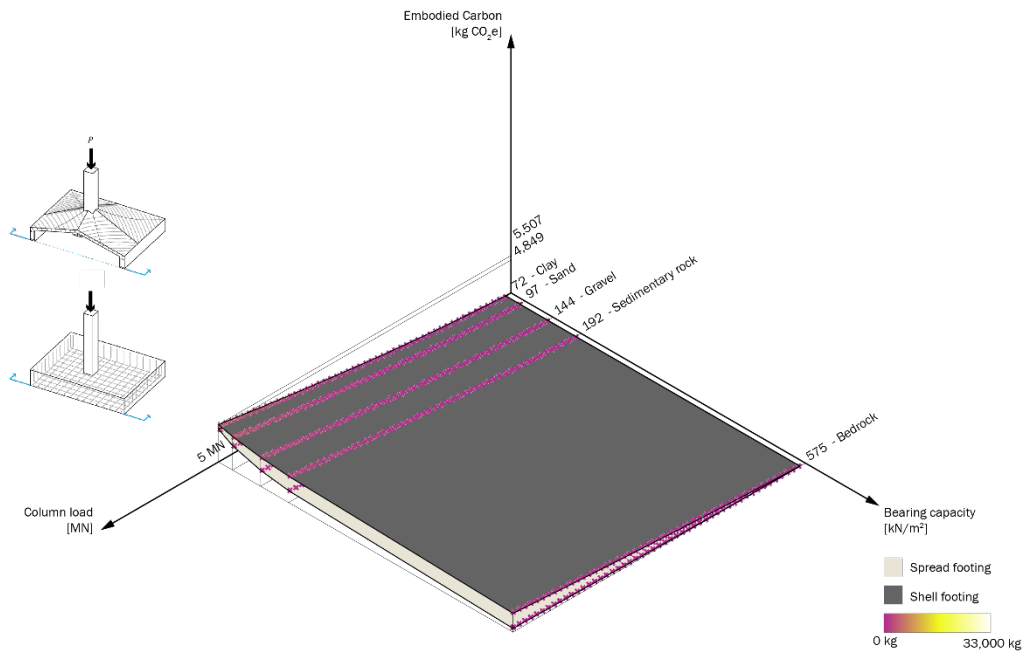
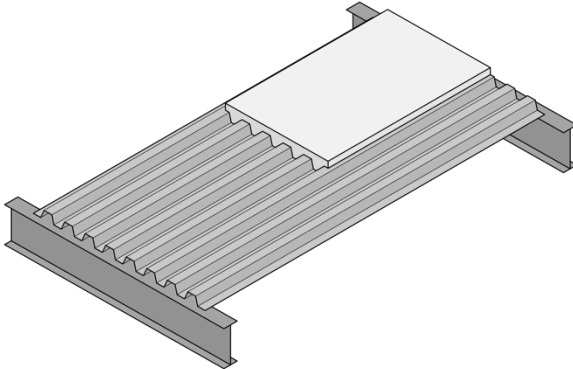

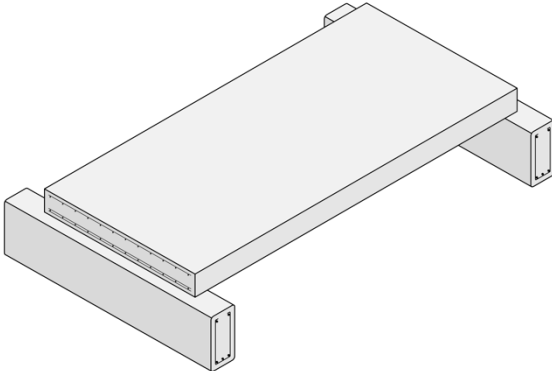
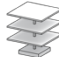
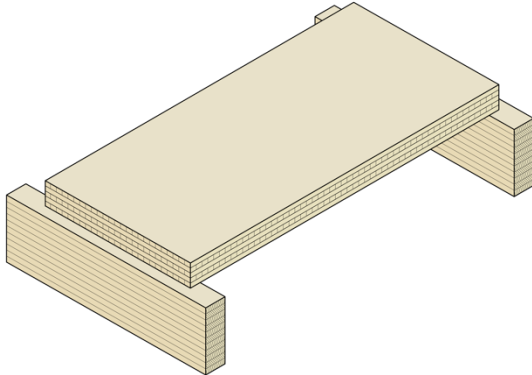



Figure 24: Partial EC contribution from steel for spread and shell footings resulting from soil bearing capacity and column load

4.1.3. NORMALIZED EMBODIED CARBON BY FOUNDATION TYPE AND FLOOR BUILD-UP IN CLAY SOIL

To assess the environmental impact of the materiality of a buildings structural system on foundations, embodied carbon values in Table 4 are divided by the floor area estimated for a 2MN load for three floor systems. As expected, due to the deadload of the systems, the concrete flat slab has the highest emissions per square meter of floor area, while the CLT slab has the lowest (Table 11). For all systems, the values are much lower than the normalized embodied carbon figures reported in Section 1.2 (Pratt 2016). This is due to the fact that only the deadload of the structural frame is being considered. When the remaining loads are added to the system, the carbon per GFA is expected to rise.

Table 11: Embodied carbon per square meter of gross floor area for a 2MN column load in clay soil

Embodied Carbon	Floor build-up:	# Floors for 2MN
Steel deck + concrete slab Spread = 17.3 kgCO ₂ e/m ² Shell = 8.9 kgCO ₂ e/m ²		 6
Concrete flat slab Spread = 34.5 kgCO ₂ e/m ² Shell = 17.8 kgCO ₂ e/m ²		 3
Cross-laminated timber (CLT) slab Spread = 8.2 kgCO ₂ e/m ² Shell = 2.0 kgCO ₂ e/m ²		 24

4.2. WHOLE BUILDING FRAME ANALYSIS

The whole building analysis evaluates how the choice of superstructure material and design impacts the carbon emissions of structural elements that are downstream in the load path. Since a building's structural elements are interrelated, the choice of superstructure material and its' geometry has a direct impact on the loads being supported by the foundations. If large-scale material savings are desired to limit carbon emissions, structural systems must be considered holistically.

4.2.1. IMPACT OF SHAPE-OPTIMIZING STRUCTURAL ELEMENTS ON GLOBAL WARMING POTENTIAL

Floor slabs contribute the majority of the embodied carbon of the upstream structural elements. If they are shape-optimized in isolation, a reduction in the structures GWP of 64% is achieved (for clay soils, $q=72\text{kN/m}^2$). By optimizing beams (in isolation), a reduction of 4% GWP is achieved and just utilizing shell foundations saves 20% GWP (See Fig. 25).

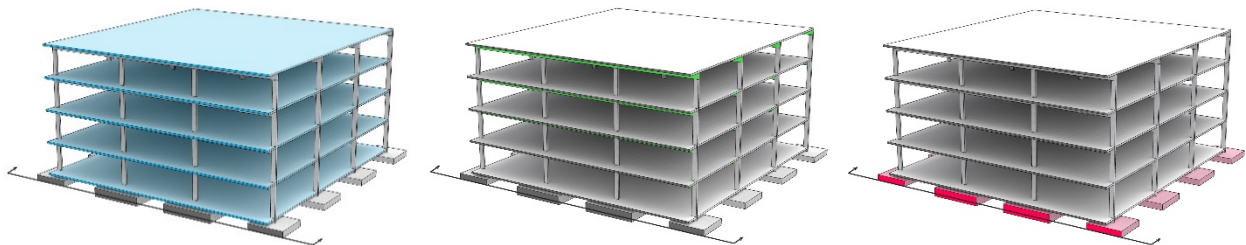


Figure 25: Structural systems that typically work in bending (a) Flat one-way spanning floor slabs (b) Beams (c) Spread footings

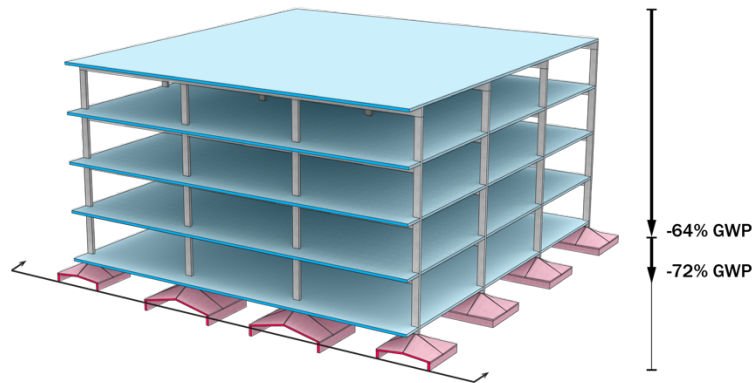


Figure 26: Global warming potential savings with optimized floor slabs and shell foundations

However, if multiple structural elements are shape-optimized, the weight of the individual components is reduced, ultimately reducing the loads being transferred to downstream elements. As foundations are the last element in the load path, acting to resolve the weight of the building to the soil below, the demand on the foundations is reduced substantially if systems are optimized upstream. As the floors and foundations contribute the majority of carbon emissions in the structural frame, the potential saving of optimizing these systems in combination is studied. In clay soils, shape optimizing floor slabs can save ~64% of a building's global warming potential. If shell foundations are implemented instead of spread footings, an additional ~8% saving is achieved (See Fig. 26), constituting a total reduction of 72% GWP. However, for high bearing capacity soils, such as sedimentary rock, no additional saving is achieved if shell foundations are implemented.

4.2.2. IMPACT OF CONCRETE STRENGTH ON REDUCING BUILDING FRAME GWP

The impact of concrete strength is also studied to determine if additional carbon savings can be achieved when various structural elements are shape-optimized (See Fig. 27).

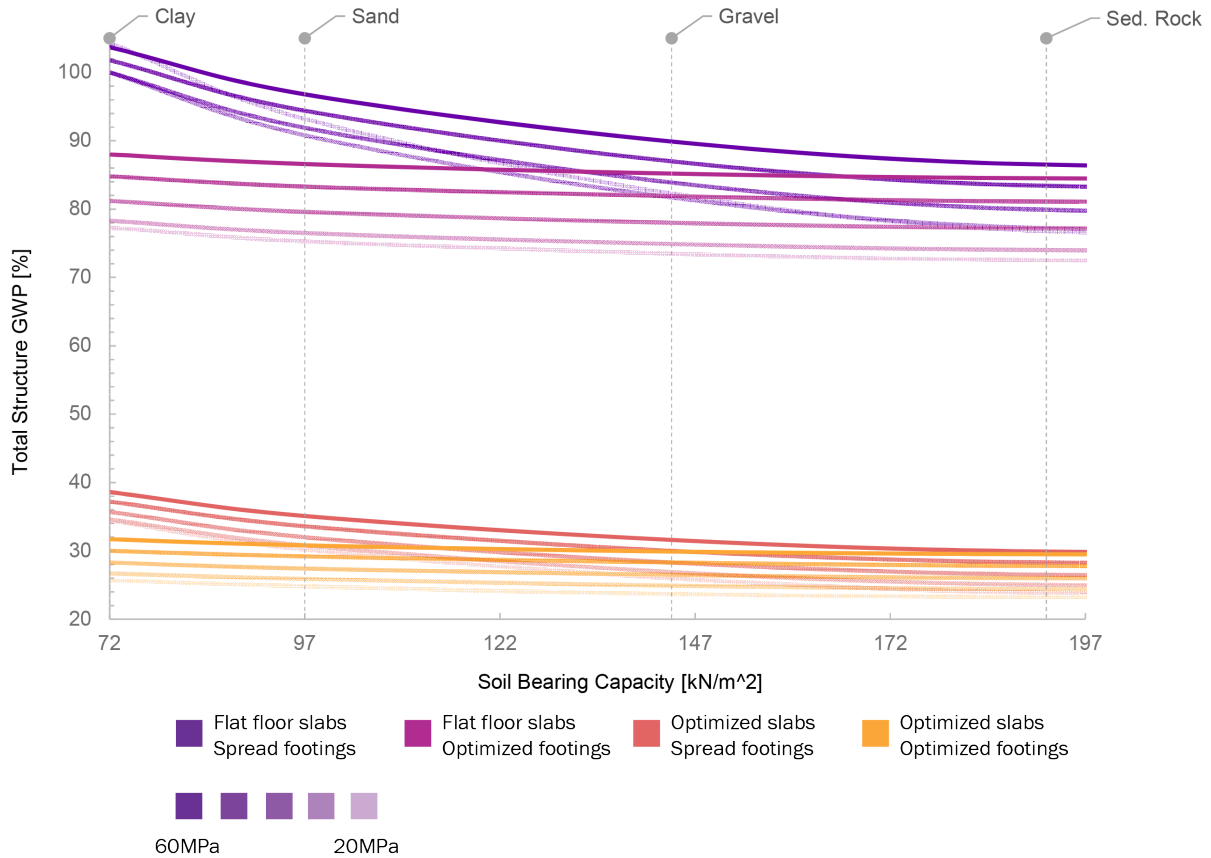


Figure 27: Impact of concrete strength and soil bearing capacity on total structural frame global warming potential for optimized floor slabs and foundations

Table 12: Impact of concrete strength on total structural frame global warming potential for clay soils for optimized floor slabs and foundations

Concrete Strength	Embodied Carbon Coefficient	Flat floor slabs Spread footings (% GWP)	Flat floor slabs Opt. footings (% GWP)	Optimized slabs Spread footings (% GWP)	Optimized slabs Opt. footings (% GWP)
20 MPa	0.1808	104.3	77.3	34.4	25.7
30 MPa	0.2288	100	78.3	34.6	26.7
40 MPa	0.2768	100	81.2	35.7	28.3
50 MPa	0.3248	101.8	84.8	37.2	30
60 MPa	0.3728	103.7	88	38.6	31.7

As expected based on the results from Section 4.2.1, the most substantial GWP saving is achieved by shape-optimizing reinforced concrete floors. By combining shape optimized floor slabs with shell foundations, ~72-79% reduction in total GWP for the structural frame can be achieved for clay soils,

depending on concrete strength. In all scenarios (with the exception of flat floor slabs and spread footings for 20MPa concrete), lower strength concrete is associated with lower total emissions for the respective combinations of optimized structural elements. Since the embodied carbon of concrete increases with strength, any material reduction achieved by using higher strength concrete is offset by the increased emissions. This suggests that low strength and low embodied carbon materials may also be substituted for virgin concrete, further reducing shell foundations' total emissions. Additionally, utilizing shell foundations has the biggest impact in low bearing capacity soils, with only marginal savings achieved by implementing them in high bearing capacity soils (See Table 12).

In summary, the saving potential of utilizing shell foundations in lieu of prismatic foundations depends largely on the soil bearing capacity as well as the optimization of structural systems further upstream with concrete strength having a lesser, but notable impact.

5. DIGITAL FABRICATION EXPERIMENTS

Due to their ability to reduce embodied carbon significantly, methods for constructing shell foundations economically are studied using contemporary digital fabrication techniques.

5.1. CONCEPTS

Shell foundations have been built extensively in contexts where material costs drive total construction costs, rather than labor costs (See Sec. 2.2). Shells are able to save material (and carbon) due to their curvature and the fact that they utilize membrane action rather than bending to distribute loads. However, this curvature and the fact that they are so thin also makes them more time-consuming to construct using traditional building methods when compared to prismatic elements. Taking inspiration from the application of digital fabrication to construct complex or nonstandard geometry, additive and subtractive methods are explored.

Local earth is proposed as formwork for two reasons; 1) it eliminates the cost and carbon emissions associated with utilizing traditional formwork materials such as timber and expanded polystyrene foam, and 2) it transfers the load to the local soil below without introducing another material. This is advantageous due to the complex nature of the shell and soil interaction (See Sec. 2.3). Although these concepts are developed and tested for the application of building shell foundations, they can be applied to other structural elements with complex geometry, such as floor slabs.

5.2. METHODS

Additive (extrusion) and subtractive (milling) methods are tested to understand the applicability of these methods for fabricating concrete shells.

5.2.1. CLAY EXTRUSION

Due to advances in 3D printing earth (See Sec. 2.4), 3D printed clay is tested to act as formwork for thin concrete shells. 3D printed earth has been deployed at building scale and has the potential to achieve complex geometry while utilizing local material. To test if clay can be used to create formwork for a hyperbolic paraboloid shell, the process in Figure 28 is used. This experiment was conducted in collaboration with Laura Maria Gonzales and Alexander Curth.

5.2.1.1. PROCESS

A KUKA robot is used in conjunction with a clay extruder developed by Gonzalez and Curth for this experiment (Curth and Gonzalez 2021). A toolpath for the robot is programmed using the KUKA|prc (parametric robot control) plug-in for grasshopper. This toolpath successively adds layers of clay from a flat plane, the base of the formwork, to the doubly-curved hyperbolic paraboloid surface to fill the negative space of the desired shell. Once the toolpath is finalized, clay is mixed to a soft consistency and then loaded into the extruder (Fig. 29a). The KUKA deposits material in successive layers until the final form is achieved (Fig. 29b). The final form is then evaluated for its ability to act as formwork for concrete and a direct shear test will be performed to evaluate the strength parameters of the material to compare to local soils.

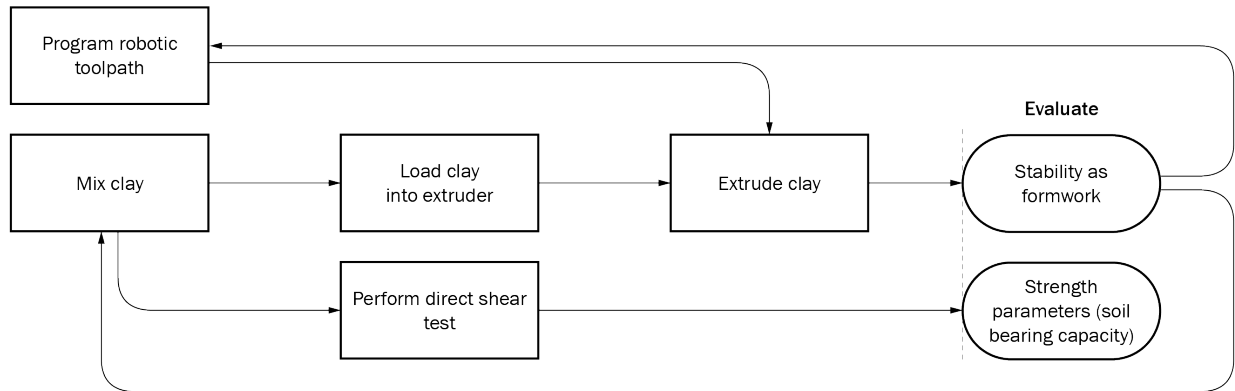


Figure 28: Methodology for 3D printing clay as formwork for thin concrete shells



Figure 29: (a) Mixing clay to load extruder, and (b) experimental set-up

5.2.1.2. OBSERVATIONS AND RESULTS

The 3D printed clay prototype can be seen in Figures 30a and 30b. This prototype measures 6 x 6" and effectively achieves the doubly-curved geometry required to construct a hyperbolic paraboloid shell (Fig 30a).

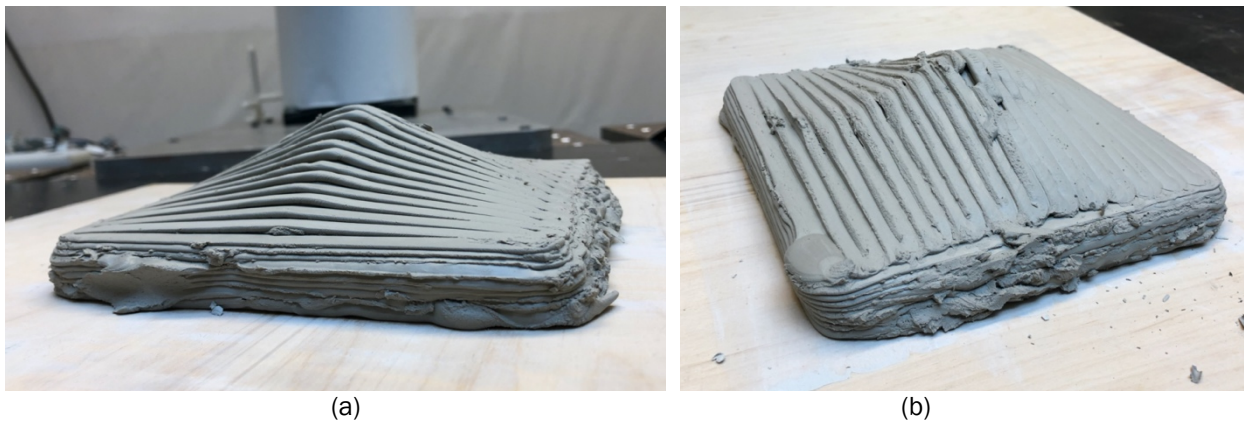


Figure 30: 3D printed clay as formwork for thin concrete shell

One limitation to this process for the application of foundations, is that the material still needs to be compacted after the geometry is extruded. Any air that is left between layers will weaken the shell/soil interface as the load is applied. If the clay is compacted after it's printed, one is not taking advantage of the precision that the robot offers. One solution is to use this process for prefabricated elements, which can be formed and then installed on site, mitigating the need for the clay to act as a load-transfer mechanism in the final state. This method can also be applied for other structural members, such as complex floor slabs, that do not need to transfer loads directly into the soil below.

Additionally, the speed that the material is deposited from the extruder remains constant. As the height of the extrusion layers is variable, further calibration of the toolpath is possible in KUKA|prc to adjust the speed of the robot to reflect the amount of material that needs to be deposited in each layer. For example, at the height of the hyper, more material needs to be deposited. The robot can be slowed in this location in order to do so.

In order to address the limitations of 3D printing clay, milling adobe is explored as an alternative method.

5.2.2. ADOBE MILLING

Milling adobe is proposed as an alternative to 3D printing clay since the material can be compacted prior to shaping it into the final form. The process for milling adobe to act as formwork in Fig. 31 is used.

5.2.2.1. PROCESS

In order to do so, a toolpath for the robot is programmed using the KUKA|prc. The KUKA robot is used in conjunction with a ceramic metal loop end-effector to successively carve the adobe mixture into the doubly-curved hyper surface for casting concrete. Once the toolpath is finalized, adobe is mixed using a 42% clay, 42% sand, 16% water mixture and loaded into timber formwork (Fig. 32a). It is then compacted using a tamp (Fig. 32b) to prepare it for milling. The KUKA traces back and forth across the adobe successively loosening material with the loop tool while a shop vacuum is simultaneously removing the loosened material until the final form is achieved (Fig. 34). Roughing passes are used (Fig. 33) to remove the initial layers with a finishing pass achieving the final geometry. This form is then evaluated for its ability to act as formwork for concrete and a direct shear test will be performed to evaluate the strength parameters of the material to compare to local soils. Concrete is then cast on the adobe formwork to create a thin shell foundation prototype.

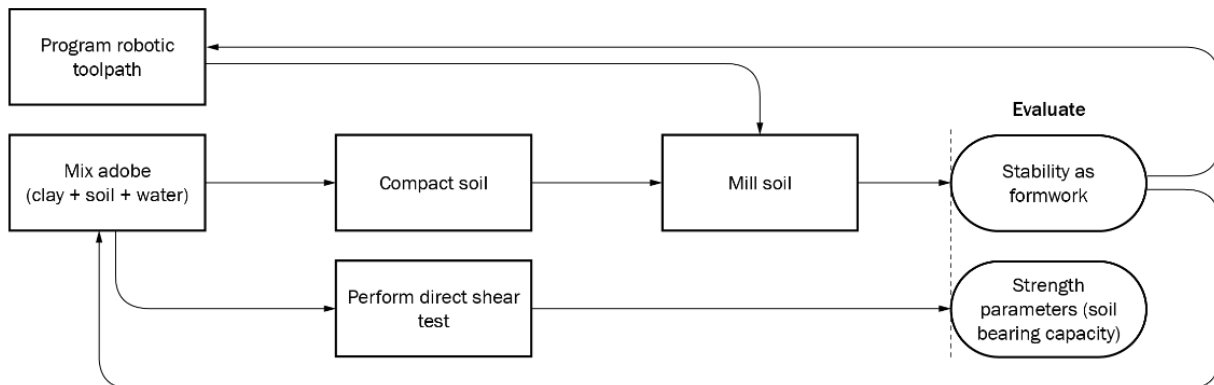
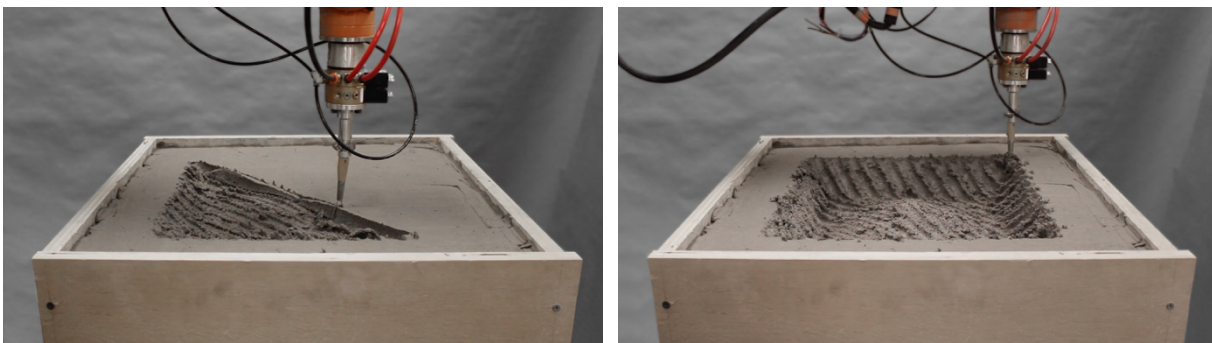


Figure 31: Methodology for milling adobe as formwork for thin concrete shells



(a) (b)

Figure 32: Tamping adobe mixture



(a) (b)

Figure 33: Robotic milling of adobe to act as formwork for thin concrete shell (a) roughing pass one, and (b) roughing pass three

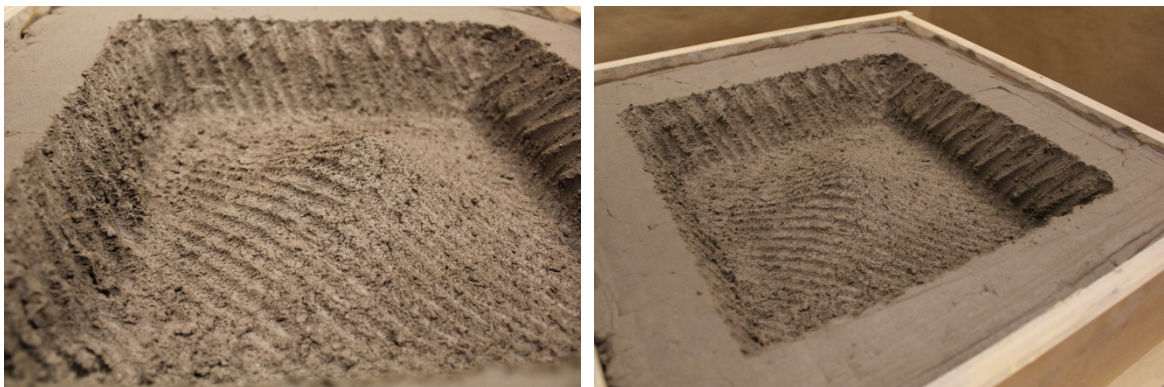


Figure 34: Final adobe formwork

Following the fabrication of the formwork, concrete is cast on the adobe to create a thin shell foundation. First, timber formwork is added to the perimeter of the shell and a layer of plastic is added to ensure the adobe does not remove moisture from the concrete as it's curing which may cause it to crack (Fig. 35a). As concrete is applied, the thickness is checked with a 3D printed template (Fig. 35b) to ensure uniform thickness. After the first layer of concrete is applied, reinforcing bars are evenly spaced with rebar chairs inserted into the clay to keep them in place (Fig.

36). Concrete is then spread evenly on top of the reinforcing bars (Fig. 37a) until the formwork is coated with an even thickness of concrete (Fig. 37b).



Figure 35: (a) Applying concrete to adobe formwork, and (b) measuring thickness of first layer



Figure 36: Adding rebar to thin concrete shell on adobe formwork



Figure 37: (a) Applying top layer of concrete, and (b) finished concrete shell on adobe formwork

5.2.2.2. OBSERVATION AND RESULTS

The resulting thin concrete shell foundation (9 x 9") can be seen in Figure 38. Milling adobe also effectively achieves the doubly-curved geometry required to construct a hyperbolic paraboloid shell, but also allows for the material to be compacted prior to fabricating the final form. This process can be scaled up using autonomous robots and larger scale end-effectors either to route or scrape the material into place in a similar manner as proposed here. Challenges that were experienced at this scale, such as creating rebar chairs for the reinforcement within a shell thickness of approximately 3/8", are not necessarily applicable at building scale. However, challenges such as the potential for the adobe mixture to dry out the concrete during curing is applicable at building scale and needs to be considered. The surface roughness generated from the loop may also improve the shell/soil interface, but needs to be studied in more detail.



Figure 38: (a) Side view of cured concrete shell foundation, and (b) cured concrete shell on adobe formwork

5.3. DIGITAL FABRICATION CONCLUSION

Digital fabrication methods, such as robotic milling, offer a pathway to economically fabricate shell foundations in contexts where the complex geometry may be too expensive to currently build. An opportunity that can be utilized in fabricating foundations, is using earth as formwork, which has a low financial and environmental cost. However, using earth also presents challenges. It must be compacted to effectively transfer building loads to the soil below, which can undermine the precise geometry created from 3D printing it. By compacting adobe and then milling it, instead, local material can be used in locations where the raw materials to make it (clay and sand) are prevalent.

6. CONCLUSION

The purpose of this thesis is to identify and characterize the opportunities that shell foundations offer for today's climate crisis and encourage architects and structural engineers to revisit shell foundations as a means to reduce material consumption in building structures.

Business-as-usual construction practices have led the building sector to contribute 11% of today's CO₂ emissions in the form of embodied carbon. These practices must be reconsidered, and alternative methods must be proposed in order to meet targets of decarbonization and to limit global warming. As foundations contribute a significant percentage of a building's total embodied carbon, 27.3% on average (Pratt 2016), shell foundations are proposed to limit carbon emissions. Shells utilize efficient geometry to transmit loads to the soil and reduce material consumption in foundations significantly. By limiting emissions, more floor area can be built while addressing the need for a significant increase in adequate housing due to rapid urbanization.

6.1. SUMMARY OF CONTRIBUTIONS

The contributions of this thesis can be summarized as:

- The application of physics-based calculations in a parametric workflow to quantify materials and compare the resulting environmental impact of prismatic (spread) foundations compared to shell foundations for the same design load and soil type. This workflow is distinct because embodied carbon takedown is typically performed at the end of the project, whereas here, it can be implemented at the design stage.
- Generalized data to determine the applicability of shell foundations to various building typologies and site conditions. By employing the parametric workflow systematically, shells were found to outperform spread footings particularly in low bearing capacity soils with the greatest CO_{2e} savings at higher applied loads.
- The extent of global warming potential savings that can be achieved by shape-optimizing multiple structural elements. When efficient foundation geometry is combined with shape-optimized floor slabs, a total GWP saving of 72% is possible in clay soils.
- The impact of concrete strength on reducing global warming potential for the structural frame. By using high strength concrete, carbon savings are reduced by 7% compared to low strength concrete.
- A method for fabricating doubly-curved concrete shells using robotically milled adobe.

6.2. POTENTIAL IMPACT

This research demonstrates that if materially efficient foundations are used in lieu of typical prismatic foundations, embodied carbon savings in excess of 60% can be achieved. Foundations are a hidden source of carbon emissions in our buildings, however, if global warming is to be limited, we must consider their impact. This work demonstrates that material consumption and the resulting carbon emissions of building foundations depends on the bearing capacity of the soil and the load applied from the building above. If disseminated, this workflow could allow designers to understand the impacts of their building design on the emissions from foundations, specifically, by allowing them to quickly iterate through designs by varying the structural and geotechnical conditions (in the form of column loads and bearing capacities, respectively). By integrating this workflow with the whole

structural frame model, designers are also able to understand the interactions and carbon saving potential between various structural elements, empowering them to prioritize efficient designs.

Fabricating formwork for complex shell geometry using digital fabrication also provides a pathway to implement thin shell foundations in locations where labor costs typically outweigh material costs. By promoting efficient geometry, significant carbon savings can be achieved, reducing the impact of business-as-usual construction methods while providing sufficient floor area for the growing global population.

6.3. LIMITATIONS AND FUTURE WORK

The work presented here evaluates isolated thin shell foundations against one typology of typical shallow foundations that work in bending, the spread footing. There is the potential to expand this investigation to other typologies, including friction piles, which do not work in bending. Additionally, the optimization of the shell shape through form-finding could lead to additional carbon savings and warrants further exploration. Alternative reinforcement that doesn't require substantial cover from concrete may greatly reduce total concrete consumption in the shell, further taking advantage of its efficient geometry. This also has the potential to extend the applicability of shells to more high bearing capacity soils and low column loads, where spread foundations currently outperform them. The interaction between multiple shells in a linear or mat arrangement could also provide additional structural and material reduction benefits. Additionally, this study can be extended to lower strength or reclaimed materials, which have the potential to further reduce emissions associated with foundations.

In practice today, design teams rely on site-specific stratification surveys provided by geotechnical engineers to engineer custom foundations for individual projects, rarely with consideration of carbon minimization strategies. In developing regions, site-specific geotechnical information can be expensive or difficult to access. Therefore, conservative assumptions are often used to design foundations, resulting in overly material intensive solutions that incur significant economic and environmental costs. This work aims to establish a workflow that can be deployed to make data-driven assessments of where emissions savings can be achieved economically through shape optimization of foundations and other structural elements, depending on site conditions. Therefore, identifying where materially efficient foundations and related technologies have the largest emissions saving potential by linking this workflow to site-specific geotechnical data is an opportunity to promote urban growth while reducing environmental impact.

6.4. CONCLUDING REMARK

Since construction will necessarily continue at high rates to meet global demand, alternative building methods must be explored to limit carbon emissions in the building sector. By highlighting the costly impact of foundations, this work seeks to encourage architects and engineers to more holistically understand and quantify the potential impact of our design choices on the environment. Substantial carbon savings are possible, today, using geometry that efficiently uses material only where structurally necessary. Although these forms are more complex than the geometries that are typically built, the potential to save a significant portion of a building's embodied carbon warrants their consideration.

REFERENCES

- Abdel-Rahman, Mohamed. 1996. "Geotechnical Behavior of Shell Foundations." Doctor of Philosophy Thesis, Department of Civil Engineering, Concordia University.
- Abergel, Thibaut, Brian Dean, John Dulac, and UN Environment and International Energy Agency. 2017. "Towards a Zero-Emission, Efficient, and Resilient Buildings and Construction Sector. Global Status Report 2017."
- "Achieving Net Zero Embodied Carbon in Structural Materials by 2050." 2020.
- Adams, Matthew, Victoria Burrows, and Stephen Richardson. 2019. "Bringing Embodied Carbon Upfront: Coordinated Action for the Building and Construction Sector to Tackle Embodied Carbon." World Green Building Council.
- Afzal, Muhammad, Yuhan Liu, Jack C.P. Cheng, and Vincent J.L. Gan. 2020. "Reinforced Concrete Structural Design Optimization: A Critical Review." *Journal of Cleaner Production* 260 (July): 120623. <https://doi.org/10.1016/j.jclepro.2020.120623>.
- Allwood, Julian M., and Jonathan M. Cullen. 2015. *Sustainable Materials Without the Hot Air: Making Buildings, Vehicles & Products Efficiently and with Less New Material*. UIT Cambridge Ltd.
- American Institute of Architects. 2021. "2030 by the Numbers: The 2020 Summary of the AIA 2030 Commitment." https://content.aia.org/sites/default/files/2022-04/2020_By_the_Numbers_AIA_2030_Commitment_Final.pdf.
- ArquitecturaViva. n.d. "Teshima Art Museum, Kagawa - Office of Ryue Nishizawa." Arquitectura Viva. Accessed April 14, 2021. <https://arquitecturaviva.com/works/museo-de-arte-teshima-4>.
- ASCE, "Arthur Casagrande | ASCE," *American Society of Civil Engineers: Bio*. <https://www.asce.org/templates/person-bio-detail.aspx?id=9915> (accessed Apr. 12, 2021).
- Block, P., T. Van Mele, M. Rippmann, and N. Paulson. 2017. *Beyond Bending - Reimagining Compression Shells*. Munich: Edition DETAIL.
- Bureau of Indian Standards. 2000. "IS 456: Plain and Reinforced Concrete - Code of Practice."
- Camp, Charles V., and Andrew Assadollahi. 2013. "CO₂ and Cost Optimization of Reinforced Concrete Footings Using a Hybrid Big Bang-Big Crunch Algorithm." *Structural and Multidisciplinary Optimization* 48 (2): 411–26. <https://doi.org/10.1007/s00158-013-0897-6>.
- Candela, Felix. 1955. "Structural Applications of Hyperbolic Paraboloidal Shells." *ACI Structural Journal* 51 (1): 397–416.
- Chiang, Yu-Chou, Pim Buskermolen, and Andrew Borgart. 2020. *Discretised Airy Stress Functions and Body Forces*.
- Cooper, Daniel R., and Timothy G. Gutowski. 2017. "The Environmental Impacts of Reuse: A Review." *Journal of Industrial Ecology* 21 (1): 38–56. <https://doi.org/10.1111/jiec.12388>.
- Curth, Alexander, Barrak Darweesh, Logman Arja, and Ronald Rael. 2020. "Advances in 3D Printed Earth Architecture: On-Site Prototyping with Local Materials." In . TU Darmstadt.
- Curth, Alexander, and Laura Gonzalez. 2021. "Extruder V1." How to Make Something that Makes (almost) Anything MAS.865. *Rapid-Prototyping of Rapid-Prototyping Machines* (blog). 2021.
- Das, Monoj Kanti. 1989. "Three Dimensional Finite Element Model to Study the Behavior of Hyperbolic Paraboloid Shell as Foundation." Master of Science in Civil Engineering Thesis, Dhaka, Bangladesh: Bangladesh University of Engineering and Technology.
- De Wolf, Catherine Elvire Lieve. 2017. "Low Carbon Pathways for Structural Design : Embodied Life Cycle Impacts of Building Structures." Thesis, Massachusetts Institute of Technology. <http://dspace.mit.edu/handle/1721.1/111491>.
- Dubor, Alexandre, Edouard Cabay, and Angelos Chronis. 2018. "Energy Efficient Design for 3D Printed Earth Architecture." In *Humanizing Digital Reality: Design Modelling Symposium Paris 2017*, edited by Klaas De Rycke, Christoph Gengnagel, Olivier Baverel, Jane Burry, Caitlin Mueller, Minh Man Nguyen, Philippe Rahm, and Mette Ramsgaard Thomsen, 383–93. Singapore: Springer. https://doi.org/10.1007/978-981-10-6611-5_33.

- EC3, Embodied Carbon in Construction Calculator by BuildingTransparency.org
Energy Technology Policy Division. 2021. "Energy Technology Perspectives 2020." International Energy Agency Directorate on Sustainability, Technology and Outlooks.
- Faber, Colin. 1963. *Candela: The Shell Builder*. New York, NY, USA: Reinhold Publishing Corporation. <https://hdl.handle.net/2027/mdp.39015006722717>.
- Fang, Demi, Nathan Brown, Catherine De Wolf, and Caitlin Mueller. In preparation. "Strategies for Reducing Embodied Carbon in Early-Stage Structural Design: A Review."
- Feickert, Kiley, and Caitlin T Mueller. 2021. "Thin Shell Foundations: Historical Review and Future Opportunities." In *IASS Annual Symposium 2020/21*. Guilford, UK.
- Fischedick, Manfred, Joyashree Roy, Amr Abdel-Aziz, Adolf Acquaye, Julian Mark Allwood, Jean-Paul Ceron, Yong Geng, et al. 2014. "Industry." In *Climate Change 2014: Mitigation of Climate Change. Contribution of Working Group III to the Fifth Assessment Report of the Intergovernmental Panel on Climate Change [Edenhofer, O., R. Pichs-Madruga, Y. Sokona, E. Farahani, S. Kadner, K. Seyboth, A. Adler, I. Baum, S. Brunner, P. Eickemeier, B. Kriemann, J. Savolainen, S. Schlömer, C. von Stechow, T. Zwickel and J.C. Minx (Eds.)]*. Cambridge University Press, Cambridge, United Kingdom and New York, NY, USA.
- García de Soto, Borja, Isolda Agustí-Juan, Jens Hunhevicz, Samuel Joss, Konrad Graser, Guillaume Habert, and Bryan T. Adey. 2018. "Productivity of Digital Fabrication in Construction: Cost and Time Analysis of a Robotically Built Wall." *Automation in Construction* 92 (August): 297–311. <https://doi.org/10.1016/j.autcon.2018.04.004>.
- Gericke, Oliver, Daria Kovaleva, Walter Haase, and Werner Sobek. 2016. "Fabrication of Concrete Parts Using a Frozen Sand Formwork." In *Spatial Structures in the 21st Century*. Tokyo. https://www.researchgate.net/publication/309464716_Fabrication_of_Concrete_Parts_using_a_Frozen_Sand_Formwork.
- Hammond, Geoff, and Craig Jones. 2008. "Inventory of Carbon & Energy (ICE)."
- Hawkins, Will, John Orr, Tim Ibell, and Paul Shepherd. 2020. "A Design Methodology to Reduce the Embodied Carbon of Concrete Buildings Using Thin-Shell Floors." *Engineering Structures* 207 (March): 110195. <https://doi.org/10.1016/j.engstruct.2020.110195>.
- Horton, John, San Juan Carma, and Douglas Stoesser. 2017. "The State Geologic Map Compilation (SGMC) Geodatabase of the Conterminous United States."
- Hurkxkens, Ilmar, Ammar Mirjan, Fabio Gramazio, Mathias Kohler, and Christophe Girot. 2020. "Robotic Landscapes: Designing Formation Processes for Large Scale Autonomous Earth Moving." In *Impact: Design With All Senses: Proceedings of the Design Modelling Symposium, Berlin 2019*, edited by Christoph Gengnagel, Olivier Baverel, Jane Burry, Mette Ramsgaard Thomsen, and Stefan Weinzierl. Cham: Springer International Publishing. <https://doi.org/10.1007/978-3-030-29829-6>.
- IAAC. n.d. "TerraPerforma - Institute for Advanced Architecture of Catalonia." IAAC (blog). Accessed April 14, 2021. <https://iaac.net/project/terraperforma/>.
- IIT Alumni., *Chair Professorship in Civil Department - Prof.P.C.Varghese - Joy of Giving*. Accessed April 10, 2021. <https://joyofgiving.alumni.iitm.ac.in/endowments/institute-chair/chair-professorship-in-civil-department-profpvcvarghese>
- Ismail, Mohamed, and Caitlin Mueller. 2021. "Minimizing Embodied Energy of Reinforced Concrete Floor Systems in Developing Countries through Shape Optimization." *Engineering Structures* 246 (November): 112955. <https://doi.org/10.1016/j.engstruct.2021.112955>.
- . 2022. "Outrage: Colonial Legacies of Concrete." *Architectural Review* (blog). April 14, 2022. <https://www.architectural-review.com/essays/outrage/outrage-colonial-legacies-of-concrete>.
- Kaethner, S C, and J A BurrIDGE. 2012. "Embodied CO2 of Structural Frames." *The Structural Engineer*, May, 33–40.
- Kurian, Nainan P. 2004. *Design of Foundation Systems: Principles and Practices*. 3rd ed. Alpha Science International Ltd.

- . 2006. *Shell Foundations: Geometry, Analysis, Design and Construction*. Alpha Science International Ltd.
- Miller, Sabbie A., Vanderley M. John, Sergio A. Pacca, and Arpad Horvath. 2018. “Carbon Dioxide Reduction Potential in the Global Cement Industry by 2050.” *Cement and Concrete Research*, Report of UNEP SBCI WORKING GROUP ON LOW-CO2 ECO-EFFICIENT CEMENT-BASED MATERIALS, 114 (December): 115–24.
<https://doi.org/10.1016/j.cemconres.2017.08.026>.
- Moreyra Garlock, Maria E., and David P. Billington. 2014. “Félix Candela and Heinz Isler: A Comparison of Two Structural Artists.” In *Shell Structures for Architecture: Form Finding and Optimization*. Routledge.
- Orr, John, A. P. Darby, Timothy Ibell, M. C. Evernden, and M. Otlet. 2011. “Concrete Structures Using Fabric Formwork,” April. <https://doi.org/10.17863/CAM.17019>.
- Orr, John, Michał P. Drewniok, Ian Walker, Tim Ibell, Alexander Copping, and Stephen Emmitt. 2019. “Minimising Energy in Construction: Practitioners’ Views on Material Efficiency.” *Resources, Conservation and Recycling* 140 (January): 125–36.
<https://doi.org/10.1016/j.resconrec.2018.09.015>.
- Plunkett, J William, and Caitlin T Mueller. 2015. “THIN CONCRETE SHELLS AT MIT: KRESGE AUDITORIUM AND THE 1954 CONFERENCE.” In , 9.
- Pratt, Quincy. 2016. “Material Quantities of Foundation Systems in Building Structures.” Thesis, Massachusetts Institute of Technology. <https://dspace.mit.edu/handle/1721.1/104234>.
- Rinaldi, Remo. 2012. “Inverted Shell Foundation Performance in Soil.” Ph.D. Civil Engineering, Montreal, Canada: Concordia University.
https://spectrum.library.concordia.ca/977243/1/Rinaldi_PhD_S2013.pdf.
- Sklar, Julia. 2015. “Robots Lay Three Times as Many Bricks as Construction Workers.” MIT Technology Review. September 2, 2015.
<https://www.technologyreview.com/2015/09/02/10587/robots-lay-three-times-as-many-bricks-as-construction-workers/>.
- Wang, Yu, and Fred H. Kulhawy. 2008. “Economic Design Optimization of Foundations.” *Journal of Geotechnical and Geoenvironmental Engineering* 134 (8): 1097–1105.
[https://doi.org/10.1061/\(ASCE\)1090-0241\(2008\)134:8\(1097\)](https://doi.org/10.1061/(ASCE)1090-0241(2008)134:8(1097)).
- Williams, Chris. 2014. “What Is a Shell?” In *Shell Structures for Architecture: Form Finding and Optimization*, edited by Sigrid Adriaenssens, Philippe Block, Diederik Veenendaal, and Chris Williams. London ; New York: Routledge/ Taylor & Francis Group.